Nonstructural Protein 5A Is Incorporated into Hepatitis C Virus Low-Density Particle through Interaction with Core Protein and Microtubules during Intracellular Transport

CrossMark

Chao-Kuen Lai[1,4], Vikas Saxena[1], Chung-Hsin Tseng[3], King-Song Jeng[1], Michinori Kohara[5], Michael M. C. Lai[1,2,3]*

1 Institute of Molecular Biology, Academia Sinica, Taipei, Taiwan, 2 Department of Molecular Microbiology and Immunology, University of Southern California, Los Angeles, California, United States of America, 3 Department of Microbiology and Immunology, and Center of Infectious Disease and Signaling Research, National Cheng Kung University, Tainan, Taiwan, 4 Graduate Institute of Toxicology, National Taiwan University, Taipei, Taiwan, 5 Department of Microbiology and Cell Biology, Tokyo Metropolitan Institute of Medical Science, Tokyo, Japan

Abstract

Nonstructural protein 5A (NS5A) of hepatitis C virus (HCV) serves dual functions in viral RNA replication and virus assembly. Here, we demonstrate that HCV replication complex along with NS5A and Core protein was transported to the lipid droplet (LD) through microtubules, and NS5A-Core complexes were then transported from LD through early-to-late endosomes to the plasma membrane via microtubules. Further studies by cofractionation analysis and immunoelectron microscopy of the released particles showed that NS5A-Core complexes, but not NS4B, were present in the low-density fractions, but not in the high-density fractions, of the HCV RNA-containing virions and associated with the internal virion core. Furthermore, exosomal markers CD63 and CD81 were also detected in the low-density fractions, but not in the high-density fractions. Overall, our results suggest that HCV NS5A is associated with the core of the low-density virus particles which exit the cell through a preexisting endosome/exosome pathway and may contribute to HCV natural infection.

Introduction

Hepatitis C virus (HCV) is a major causative agent of chronic hepatitis, liver cirrhosis, and hepatocellular carcinoma. HCV is an enveloped virus with a 9.6-kb positive-strand RNA genome. This genome encodes a large polyprotein, which is processed by host and viral proteases into 10 viral proteins that consist of three structural proteins, six nonstructural proteins, and a small hydrophobic peptide, p7 [1,2]. The structural proteins, Core protein and two envelope glycoproteins E1 and E2, are derived from the N terminal portion of the polyprotein and constitute physical virion components. The nonstructural (NS) proteins, NS2, NS3, NS4A, NS4B, NS5A, and NS5B, are derived from the C terminal portion of the polyprotein. Most of the NS proteins (with the exception of NS2) are involved in HCV replication [3,4]. HCV RNA is synthesized in the replication complex (RC), which exists in the membranous web derived from altered ER membranes [5,6]. The HCV RC is transported on microtubules and this transport is facilitated by the interaction of NS3 and NS5A with tubulin [7]. The intact microtubule network also is directly involved in HCV RNA replication [8–10] and virus release [10,11].

Following HCV RNA replication, Core protein and NS5A serve as central regulators of virus assembly [12]. Core protein forms multimers [13] and interacts with the viral RNA [14] to form the viral nucleocapsid. The Core protein is localized mainly on the surface of the lipid droplets (LDs) [15,16], which is essential for the production of infectious HCV particles [15]. Further, Core protein promotes the accumulation of LDs to facilitate virus assembly [11,17] and recruits viral RCs to LD-associated membranes [15]. Thereby, viral RNA interacts with Core protein in juxtaposition to LD for virus packaging. Moreover, the interaction between NS5A and Core protein is essential for the recruitment of the viral RCs to LDs and plays an important role in virus assembly [18,19]. However, how viral RCs and Core protein target to LD remains unclear. In addition to NS5A, other NS proteins, including NS2, NS3, and NS4B, have also been shown to influence the production of infectious virus [12]. Up to now, it is not known whether the NS proteins are incorporated into infectious virions.

Previous studies have indicated that cell culture- [20–24] and patients' serum-derived [25–29] HCV particles display heterogeneous diameters (from 35 to 145 nm) and have a broad range of buoyant density (between 1.01 g/ml and 1.17 g/ml). The main peak of both viral Core protein and RNA exhibited at a density of 1.15 to 1.17 g/ml in the cell culture derived-HCV (HCVcc) [30,31], and the highest specific infectivity of extracellular virion was observed at a density of 1.14 g/ml [20]. Notably, the low-density fraction (density of <1.1 g/ml) displays exosome-like

structures and also contains infectivity [20], but the nature and origin of their properties are still unknown.

Many types of cell continuously secrete a large number of microvesicles, called exosomes, which have a diameter of approximately 50–150 nm and have a buoyant density between 1.08 g/ml and 1.22 g/ml [32]. Exosomes are released into the extracellular space from late endosomes/multivesicular bodies (MVBs) fusion with the plasma membrane [33]. More recently, the exosomes derived from cells containing HCV subgenomic replicon have been demonstrated to contain HCV RNA, but not viral NS proteins [34]. Our previous results [10] have shown that HCV Core proteins are transported from early to late endosomes/MVB in HCV-infected cells. However, it is not known whether any HCV proteins are incorporated into the released exosomes from HCV-infected cells.

In this study, the trafficking mechanism of the NS5A and Core proteins is defined further. Both NS5A and Core proteins are found to be closely associated with and co-transported along the microtubules from the perinuclear region of cells via the LDs and endosomes to the plasma membrane. This association of NS5A-Core proteins implicated them in virus assembly as well as release. Interestingly, we found that both NS5A and Core, in addition to exosomal proteins CD63 and CD81, were detected in the low-density HCV particles (1.083 to 1.098 g/ml) with low-grade infectivity. NS5A appeared to be incorporated into HCV particles through interaction with Core protein and microtubules during intracellular transport. Our data suggest that NS5A-containing, low-density HCV particles were released in the form of exosome.

Materials and Methods

Cells and plasmid

Huh7.5 cells, a mutant line of Huh7 cells that support HCV replication at high efficiency [35] were cultured in Dulbecco's Modified Eagle's Medium (DMEM) containing either 10% fetal bovine serum (FBS) or 10% dialyzed FBS [36] for a general subculturing and for preparation of purified HCV, respectively. Rep 1.1 cells [7,37] are Huh7 cells that harbor a genotype 1b HCV subgenomic replicon. They were grown in the aforementioned medium containing 0.5 mg/ml of G418. Plasmid pUC-Jc1, which encodes a chimera genome of HCV J6CF/JFH1, was constructed as previously described [38].

Antibodies and reagents

Antibodies used in this study included anti-NS5A (Austral Biologicals), anti-Core (Affinity Bioreagents Inc.), anti-bromodeoxyuridine (Sigma-Aldrich), anti-EEA1 or -CD63 or -LAMP-1 (Santa Cruz Biotechnology), mouse anti-CD81 (BD Pharmingen), rabbit anti-CD81 (Santa Cruz Biotechnology), anti-E2 (GeneTex, Inc.), anti-calnexin (Assay designs/Stressgen), and anti-mouse or -rabbit colloidal gold conjugates (Jackson ImmunoResearch Inc.). Rabbit polyclonal Abs against Core (RR8) and NS4B (RR12) were described previously [15]. Cy3-conjugated primary Ab to β-tubulin and nonspecific normal mouse immunoglobulin G (IgG) were obtained from Sigma-Aldrich. Secondary Abs against mouse, rabbit and goat were purchased from Invitrogen Molecular Probes.

Reagents used were Nocodazole (Sigma-Aldrich), taxol (paclitaxel; Sigma-Aldrich), BODIPY 493/503 (Invitrogen Molecular Probes), 4',6-Diamidino-2-phenylindole (DAPI; Invitrogen Molecular Probes) and wheatgerm agglutinin (WGA) Alexa Fluor 647 conjugate (Invitrogen Molecular Probes).

Preparation of purified HCV particles

The Jc1 viruses were produced and titrated in Huh7.5 cells based on a previously described method [7]. The same batch of culture supernatant from virus-infected and the control cells, including HCV subgenomic replicon cells (HCV assembly-defective replicon cells) and uninfected cells, was used in all experiments. The concentrated HCV Jc1 and controls were subjected to 10 to 50% sucrose gradient sedimentation centrifugation as previously described [39]. A total of 15 fractions of 0.75 ml each was collected from the bottom to the top of the sucrose gradient and monitored for HCV RNA by using quantitative PCR (qPCR) [10]. Fractions containing the HCV RNA signal (fractions 7 to 8 and fractions 11 to 13) and their uninfected counterparts were pooled and dialyzed against TNE buffer (10 mM Tris, 150 mM NaCl, 2 mM ethylene diamine tetraacetic acid) overnight at 4°C. The virus-containing fractions were then concentrated by 10-fold in Ultracel-3k concentration devices (Millipore) and further processed for electron microscopy applications or infection. Infectivity of each fraction was determined by quantifying the amounts of intracellular HCV RNA levels at day 3 postinfection (p.i.).

Determination of HCV infectivity by quantitative reverse transcription-PCR (qRT-PCR) of intracellular HCV RNA of infected cells

Huh7.5 cells in six-well plates were infected with concentrated HCV from each fraction of the sucrose gradient suspended in DMEM at 37°C for 3 h. Cells were washed with PBS and incubated with 2 ml of DMEM containing 10% FBS. At 3 days postinfection, total RNA was isolated from cell lysates using a High Pure RNA isolating kit (Roche). Viral RNA was isolated from cell culture supernatants using a QIAamp viral RNA kit (Qiagen). qRT-PCR was performed as described previously [10,40].

Electron microscopy (EM)

The procedure of EM was carried out exactly as described previously [40]. For immuno-EM, samples were first incubated with an anti-NS5A, anti-Core or anti-E2 mouse MAb, and followed by incubation with colloidal gold particles of 18 nm conjugated to anti-mouse immunoglobulin G. For immuno-EM of the purified viruses, two microliters of purified virus were adsorbed onto carbon-coated grids. Grids were fixed with 2% paraformaldehyde for 10 min and blocked in a solution of 0.5% bovine serum albumin (BSA) for 20 min. The grids were incubated with primary Abs and normal mouse IgG for overnight at 4°C. Grids were then washed and incubated with goat anti-mouse and/or goat anti-rabbit colloidal gold particles (6- and 12-nm diameter) for 1 h at room temperature. After extensive washing, the grids were stained with 1% uranyl acetate for 1 min. For analysis of HCV core particle, the purified virus was treated with 0.01% saponin in PBS for 20 min before processing. All samples were analyzed under a Tecnai Spirit transmission electron microscope (FEI Co) at 120 kV.

Labeling of de novo-synthesized viral RNA

Cell labeling with 5-bromouridine 5'-triphosphate (BrUTP) was performed according to the methods described previously [7]. HCV-infected cells (at day 10 p.i.) were grown on 4-well chamber slides. One day after seeding, cells were incubated with actinomycin D (10 µg/ml) for 30 min. Then, 20 µl of BrUTP/Fugene 6 (Roche Molecular Biochemicals) mixture were added to each well containing 500 µl medium with actinomycin D (10 µg/ml). After 30 min of incubation at 37°C, cells were treated with 10 µM nocodazole or taxol for 1 h, and then fixed and processed for immunofluorescence staining as described below.
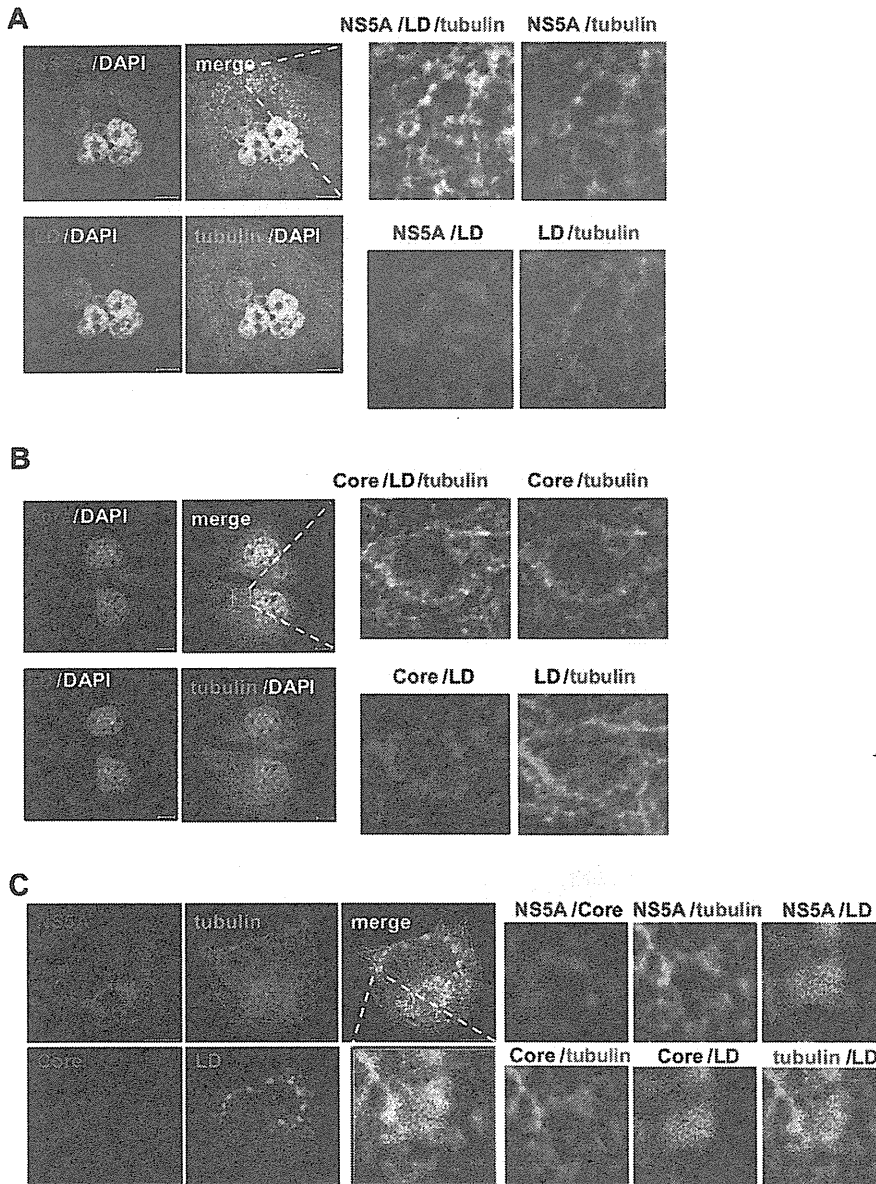
—76—

Figure 1. Colocalization of NS5A with Core protein and microtubules in lipid droplets. HCV-infected cells (at day 10 p.i.) were co-stained with anti-tubulin (green), -NS5A (red) (A) and/or -Core (red, B; blue, C) antibodies. Lipid droplets (LDs) were stained with BODYPI 493/503 (blue, A and B; brown, C) and nuclei with DAPI (gray). Stained cells were examined by confocal fluorescence microscope. Merging of the images in the green, red, blue, and gray channels generated the pictures in Fig. A and B. Fig. C was generated by merging the images in the green, red, blue, and brown channels. Yellow indicates overlapping localization of the green and red channels, cyan indicates overlapping localization of the green and blue channels, magenta indicates overlapping localization of the red and blue channels, and white indicates overlapping localization of the red, green, and blue channels. The upper third panels in Fig. A and B and the lower third panel in Fig. C are enlarged areas from the merged image. The same enlarged area is defined in terms of two proteins at a time, as indicated, in the adjoining three panels in Fig. A and B, and six panels in Fig. C. Bars, 10 μm.
doi:10.1371/journal.pone.0099022.g001

Immunofluorescence staining

Cells were gown on glass chamber slides. Cell fixation and immunostaining were performed by the methods described by Listenberger L. L. and Brown D. A. [41]. Photographs of the cells were taken with a confocal microscope (Zeiss Confocal Laser Scanning Microscope LSM 510META-NLO).

Image processing and quantitative analysis

The procedure for quantitative colocalization analysis used in this study followed the published method [10]. The weighted colocalization coefficient is the sum of intensities of colocalization pixels relative to the overall sum of pixel intensities above the threshold. It was used to determine the relative levels of
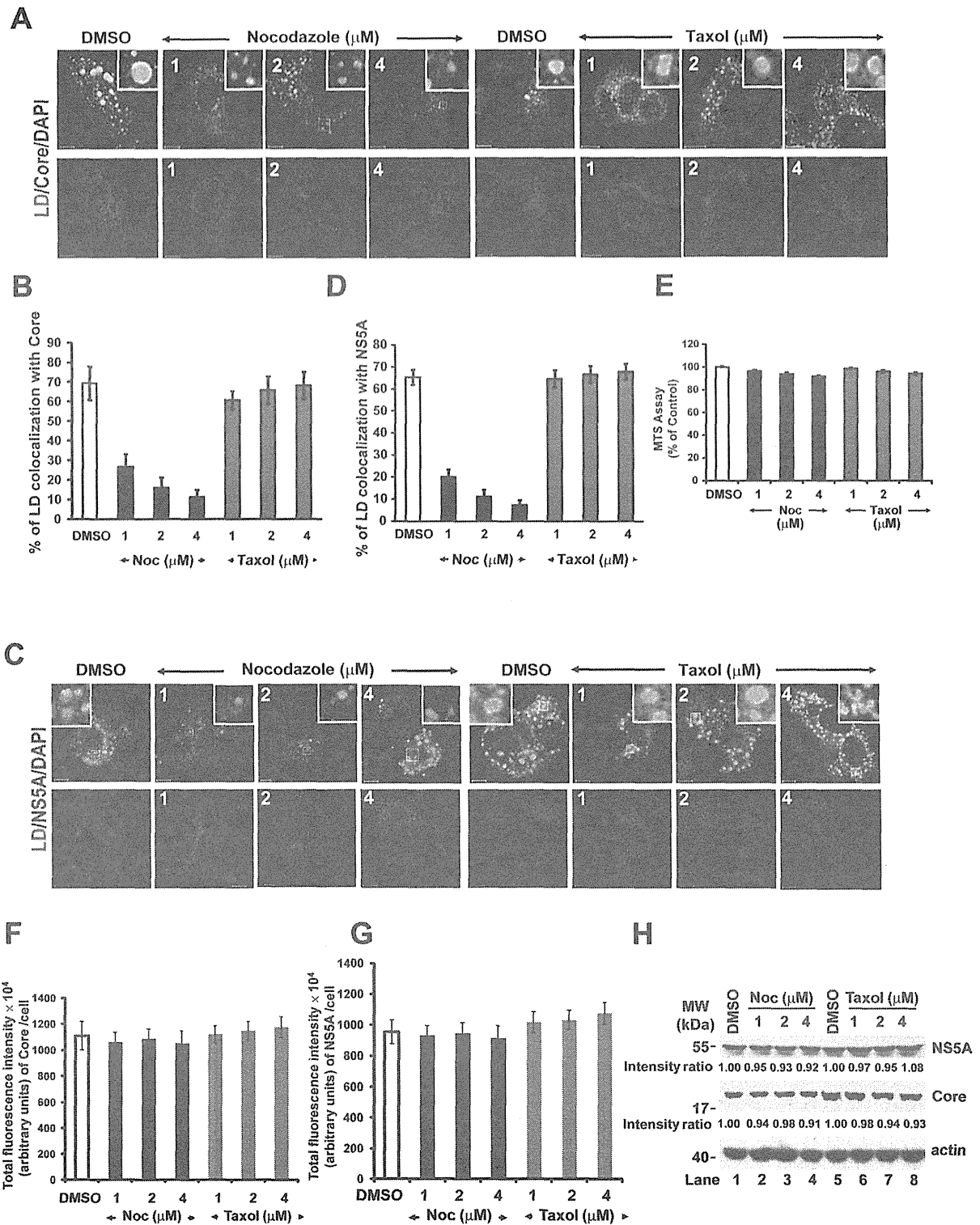
Figure 2. Nocodazole blocks the transport of NS5A and Core protein to the lipid droplet in a dose-dependent manner. Huh7.5 cells were first infected with HCV Jc1 virus at a multiplicity of infection of 0.5 for 3 h, and then the cells were treated with either nocodazole (1 to 4 µM) or taxol (1 to 4 µM) at various concentrations for 2 days. The cells were stained with anti-Core (red) (A) or -NS5A (red) (C) antibodies. LDs and nuclei were stained with BODYPI 493/503 (green) and DAPI (blue), respectively. Enlarged views of parts of every image are shown (insets). The same images are

—78—

shown for Core (red) or NS5A (red) and with DAPI (blue) in the lower panels of Fig. A and C, respectively. Colocalization efficiency between LD and Core protein (B) and between LD and NS5A (D) was analyzed by using Zeiss LSM Zen software. (E) Analysis of cellular proliferation and survival by MTS assay. (F, G) Quantitation of confocal microscopic fluorescent signals of Core and NS5A in cells. The total fluorescence intensities of Core protein and NS5A were measured using MetaMorph Integrated Morphometry Analysis. A total of 20 cells were used for calculation of colocalization efficiency and total fluorescence intensity from two independent experiments and error bars represent standard deviations of the mean. Noc, nocodazole. Bars, 10 μm. (H) In parallel, the cell lysates were collected and then immunoblotted with antibodies against Core and NS5A. Results were quantified by PhosphorImager counting.
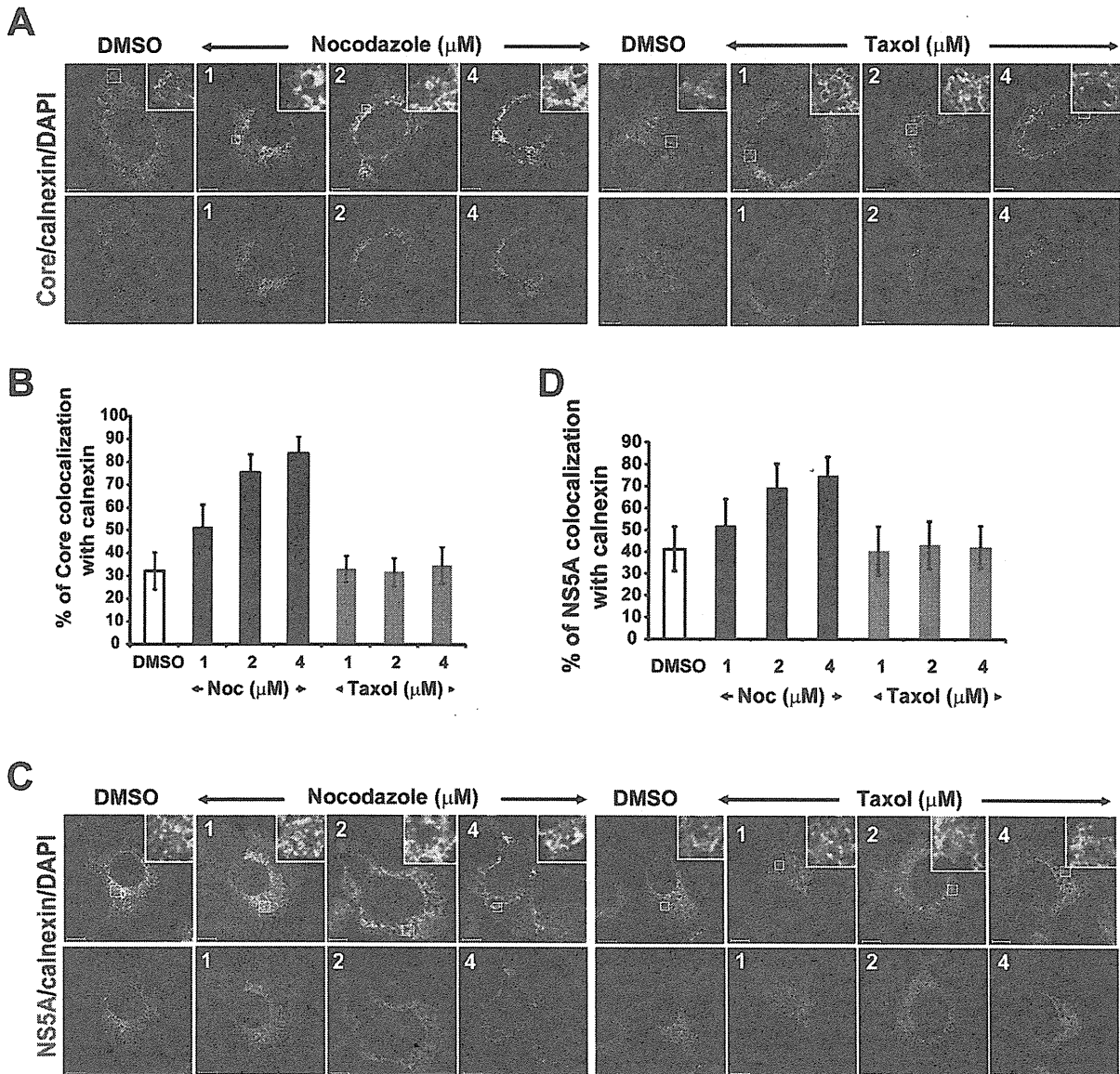doi:10.1371/journal.pone.0099022.g002

Figure 3. Effects of Nocodazole on movement of NS5A and Core protein. Huh7.5 cells were first infected with HCV Jc1 virus at a multiplicity of infection of 0.5 for 3 h, and then the cells were treated with either nocodazole (1 to 4 μM) or taxol (1 to 4 μM) at various concentrations for 2 days for the analysis of colocalization of Core protein or NS5A and calnexin. The cells were co-stained with a polyclonal antibody against calnexin (red) to visualize the ER and a MAb against Core protein (green) (A) or NS5A (green) (C). Nuclei were stained with DAPI (blue). Enlarged views of parts of every image are shown (insets). The same images are shown for Core (green) or NS5A (green) and with DAPI (blue) in the lower panels of Fig. A and C, respectively. Colocalization efficiency between Core protein and calnexin (B) and between NS5A and calnexin (D) was analyzed by using Zeiss LSM Zen software. A total of 20 cells were used for calculation of colocalization efficiency from two independent experiments and error bars represent standard deviations of the mean.
doi:10.1371/journal.pone.0099022.g003

—79—
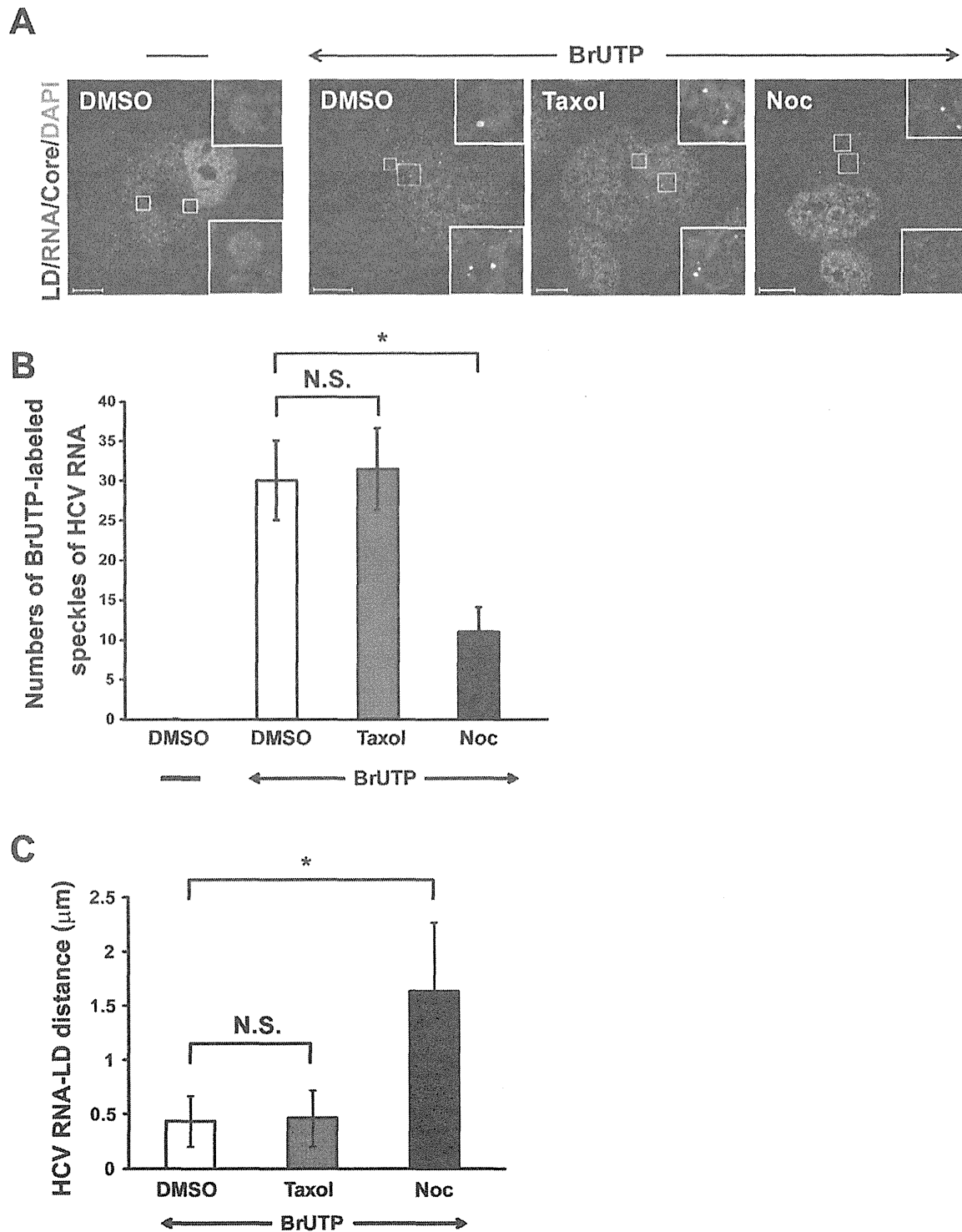
Figure 4. Nocodazole affects the movement of viral replication complexes (RCs) to the LDs. (A) The HCV-infected cells (at day 10 p.i.) were transfected with BrUTP in the presence of actinomycin D for 1 h and then treated with either 10 μM nocodazole or 10 μM taxol for 1 h. The cells were co-stained with mouse MAb against bromodeoxyuridine (green) and rabbit polyclonal antibodies against Core (RR8) (red). LDs and nuclei were stained with BODYPI 493/503 (blue) and DAPI (cyan), respectively. Enlarged views of parts of every image are shown (insets). (B) The number of BrUTP-labeled viral RNA was counted manually using an original magnification of ×630 and followed by a quantitation analysis performed by an observer blinded to the experimental treatment. (C) The average distance between the center of the signal emitted by the BrUTP-labeled viral RNA

−80−

colocalization between Core protein, NS5A or NS4B with the protein of interest (e.g., calnexin, LD). The shortest and longest average distances between the BrUTP-labeled viral RNA signal center and the nearest edge of LD were calculated manually using ZEN software (Zen 2009 light edition; Carl Zeiss Inc). The number of BrUTP-labeled viral RNA and antibody-labeled signals of viral proteins at the plasma membrane was manually counted in an original magnification of 630. Total fluorescence intensity values of Core protein and NS5A for individual cells were measured using the MetaMorph software (Universal Imaging Corporation), using 8 bit images. The gray-scale of the 8-bit images ranged from 0 (black) to 256 (white). Image analysis was carried out using the Integrated Morphometry Analysis program provided by MetaMorph. Fluorescence intensity is expressed as the integrated value of all pixels per cell that exceed the inclusive threshold value set at 40. A total of 20 cells were used in each experimental condition from two independent experiments.

MTS assay

A CellTiter96A$_{Queous}$ One solution cell proliferation assay kit (Promega) was used to evaluate cell viability, which was performed as described previously [40].

Results

HCV NS5A colocalizes with Core protein on lipid droplet, and the complex is closely associated with microtubules

Our previous studies have shown that microtubule provides the track for the movement of HCV RCs through NS5A-microtubule interaction [7] and that this transport is required for virus release [10]. We propose that microtubules also provide tracks for the transport of NS5A or the NS5A-containing RC and Core protein to reach the LD, where virus assembly occurs. To test this possibility, we first investigated whether Core-containing LDs colocalized with NS5A and associated with microtubules in HCV-infected Huh7.5 cells [at day 10 postinfection (p.i.)]. Immunofluorescence staining revealed that NS5A and Core protein together (Fig. 1C), or either one alone (Fig. 1A and 1B), is colocalized on the surface of LD and is closely associated with tubulins.

The microtubule network is required for the trafficking of NS5A or the NS5A-containing replication complexes and Core protein to the lipid droplet

We used nocodazole (which induces microtubule depolymerization) or taxol (which stabilizes tubulin polymerization) to examine whether intact microtubules are required for the transport of Core protein, NS5A or viral RCs to the LD. Huh7.5 cells were first infected with HCV, and treated with either nocodazole or taxol at 3 hr p.i. for 2 days. The colocalization coefficient of LD with Core protein or NS5A was then calculated. Under these conditions, cell viability was not affected, as revealed by 3-(4,5-dimethylthiazol-2-yl)-5-(3-carboxymethoxyphenyl)-2-(4-sulfophenyl)-2H-tetrazolium salt (MTS) assay (Fig. 2E).

Under the control conditions [dimethyl sulfoxide (DMSO)], LD colocalized with Core protein throughout the entire cytoplasm, including the perinuclear region; the proportion of LD that colocalized with Core protein was 69%. When the cells were treated with increasing concentrations of nocodazole, a dose-

dependent decrease in the colocalization coefficient of LD with Core protein was observed (Fig. 2A upper panels and 2B). The colocalization coefficient of LD with NS5A also decreased correspondingly (Fig. 2C upper panels and 2D). Taxol did not have effects on this coefficient. In order to rule out the possibility that the dose-dependent decrease in the colocalization of LD with Core or NS5A by nocodazole treatments might have been the consequence of a decrease in the amounts of Core and NS5A proteins, a further analysis of Core protein (Fig. 2A and 3A, lower panels) and NS5A (Fig. 2C and 3C, lower panels) labeling in cells was carried out using the MetaMorph Integrated Morphometry Analysis. In nocodazole-treated cells, there was no significant change on the total fluorescence intensities of Core and NS5A relative to control cells (Fig. 2F and 2G). Immunoblot analysis also showed that the levels of NS5A and Core proteins in the cells were not significantly affected by the low concentration (up to 4 μM) of nocodazole or taxol used (Fig. 2H,). This was in contrast to the effects of nocodazole at 10 or more μM used in most of the published studies, which inhibited HCV RNA replication and thereby HCV protein level [8,10,42]. These data support the conclusion that the nocodazole treatment at low concentrations affected the colocalization of Core and NS5A with LD (Fig. 2B and Fig. 2D). Taken together, these results indicated that microtubules are involved in the transport of Core protein and NS5A to the LD.

Newly synthesized membrane proteins generally leave the endoplasmic reticulum (ER) and transported to other destinations in the cells. Therefore, we next investigated whether NS5A and Core proteins are transported from ER to LDs along the microtubules. In the presence of DMSO or taxol, Core protein was colocalized with the ER marker protein calnexin throughout the entire cytoplasm, including the perinuclear region, with a colocalization coefficient of 32% (Fig. 3A and 3B). In contrast, the nocodazole treatment caused a dose-dependent increase of colocalization coefficient to 75% and 84% at 2 and 4 μM nocodazole, respectively (Fig. 3A, upper panels and 3B). Similarly, the colocalization coefficient of NS5A with calnexin increased from 41% to 69% and 75%, respectively (Fig. 3C, upper panels and 3D). Thus, the nocodazole treatment caused an increased accumulation of Core protein and NS5A in the ER and corresponding decrease in the LDs. Taken together, these results suggested that NS5A and Core protein are translocated from ER to LDs in a microtubule-dependent manner.

We further confirmed the mode of transportation of the HCV RC to the LD by immunofluorescent labeling of newly synthesized HCV RNA with BrUTP [43]. In the DMSO control and taxol-treated cells, the number of BrUTP-labeled speckles averaged 30 per cell, and the average distance between speckle and LD was 0.43 μm (Fig. 4). In the presence of nocodazole, the number of speckles was reduced to an average of 11 per cell (Fig. 4B), indicating that the HCV RNA replication is partially suppressed by nocodazole treatments, consistent with the previous reports [8–10]. Correspondingly, the average distance between the speckle center and the nearest edge of LD increased from 0.43 μm in the DMSO controls and taxol-treated cells to 1.63 μm in the nocodazole-treated cells (Fig. 4C), suggesting that the HCV RCs are normally delivered to the vicinity of the LDs through microtubule and that this transport is disrupted by nocodazole. Taken together, these data suggest that NS5A or the NS5A-
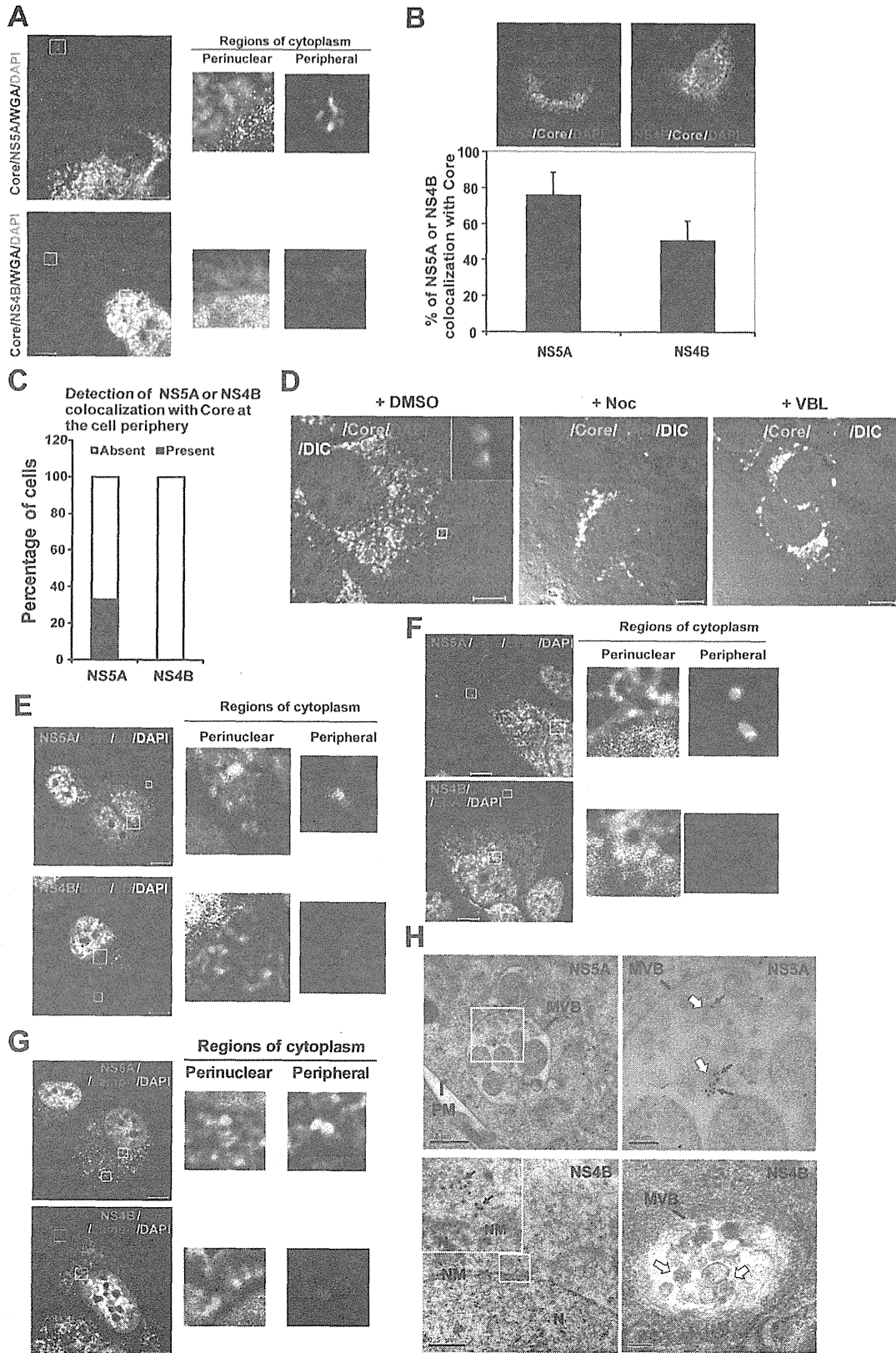
-81-

Figure 5. Core-NS5A complexes are transported from perinuclear region to early and late endosomes. (A) The HCV-infected cells (at day 10 p.i.) were labeled with antibodies specific for Core protein (red) and NS5A (green) (upper row) or NS4B (green) (lower row). Plasma membrane and nuclei were stained with WGA Alexa Fluor 647 conjugate (blue) and DAPI (gray), respectively. In parallel with panel A, the HCV-infected cells were labeled with antibodies to Core protein (green) and NS5A (red) or NS4B (red) (B, upper rows). Nuclei were stained with DAPI (blue). Colocalization efficiency between Core protein and NS5A or NS4B was analyzed by using Zeiss LSM Zen software (B, lower panel). Error bars represent standard deviations of the mean from 20 cells in two independent experiments. The images were analyzed by using MetaMorph, and the proportion of cells (of 200 counted) in which the NS5A or NS4B colocalized with Core protein at the cell periphery was calculated (C). (D) Effects of nocodazole (Noc) and vinblastine (VBL) on movement of Core-NS5A protein complex to the cell periphery. The HCV-infected cells (at day 10 p.i.) were treated with nocodazole, vinblastine, or DMSO for 3 h. The cells were labeled with antibodies to Core protein (green), NS5A (red). Nuclei were stained with DAPI (blue). Images with differential interference contrast (DIC) and fluorescence images were then merged. An enlarged view of part of image is shown (inset). In parallel with panel A, the HCV-infected cells were labeled with antibodies to Core protein (red) (E, F, G), NS5A (green, E, F, G) (upper rows), NS4B (green, E, F, G) (lower rows), EEA1 (blue) (F) and Lamp-1 (blue) (G). LDs and nuclei were stained with BODYPI 493/503 (blue) (E) and DAPI (gray), respectively. The second and third panels in each row are magnified views, marked with a white box in the panel at the extreme left, of the perinuclear and the peripheral regions of cytoplasm, respectively (A, E, F, G). Colocalization of Core protein with NS5A or NS4B is depicted as yellow (A, B, D, E, F, G). Colocalization of Core-NS5A or -NS4B complexes with LDs (E), early endosomes (F) or late endosomes (G) is depicted as white. Bars, 10 μm. (H) In parallel, the HCV-infected cells was labeled with anti-NS5A or -NS4B Ab. Bound antibodies were detected using anti-mouse or -rabbit secondary antibodies conjugated to 18- or 12-nm gold particles, respectively. Sections were visualized by EM. Arrows, gold-labeled NS5A (18 nm) and NS4B (12 nm) are indicated. MVB contains several intravesicular vesicles (white arrows). An enlarged view of the perinuclear region of lower left image is shown (inset). Arrows, gold-labeled NS5A and NS4B. PM, plasma membrane; MVB, multivesicular bodies; N, nucleus; NM, nuclear membrane; Bars, 500 nm (left panels) and 100 nm (right panels).
doi:10.1371/journal.pone.0099022.g005

containing replication complexes and Core protein are transported to the LDs through microtubules.

NS5A and Core protein complex is cotransported from the perinuclear region to the plasma membrane via microtubule

NS5A, together with Core protein, is involved in virus assembly; the assembled virions are presumably transported to the plasma membrane to be released off the cell. Therefore, we next analyzed whether NS5A is involved in the post-assembly processes of viral life cycle. For this purpose, we examined the colocalization of NS5A with Core protein in two regions of the cytoplasm, viz. the perinuclear (region just around the nucleus) and the peripheral (region just underneath the plasma membrane) regions. HCV-infected cells were co-stained with fluorescent (Alexa 647) WGA (which binds glycoproteins on the cell membrane), which serves as a membrane marker, anti-Core, and either anti-NS5A or -NS4B Abs. As shown in Fig. 5A, NS5A and Core protein colocalized both in the perinuclear region and at the cell periphery. In contrast, NS4B colocalized with the Core protein only in the perinuclear region of cytoplasm, but not in the peripheral region. Analysis of a large number of cells indicated that Core protein was colocalized with NS5A throughout the entire cytoplasm, but not with NS4B (Fig. 5B, upper panels). The total fraction of NS5A that colocalized with Core protein was 76%, while the corresponding NS4B was 51% (Fig. 5B, lower panel). Further, the NS5A-Core complex colocalized in the peripheral region in 33% of the cells, whereas NS4B-Core did not colocalize at all in the same region (Fig. 5C). We next examined the possibility that the Core-NS5A complexes are also transported along microtubule to the cell periphery. In the DMSO-treated cells, NS5A colocalized with Core protein in both the perinuclear and peripheral regions (Fig.5D). After treatment with either nocodazole or vinblastine, the Core-NS5A complexes clustered almost exclusively in the perinuclear region (Fig. 5D). These results suggested that microtubules are required for the transport of Core-NS5A complexes to the cell periphery. This observation further suggests that NS5A, but not NS4B, is involved in the post-assembly transport of virus particles.

To further evaluate the involvement of the NS5A-Core complex in HCV assembly and release, we investigated the localization of this complex with respect to LDs [15], early and late endosomes [10,44–47], and microtubules [10,11], all of which are involved in the various steps of HCV assembly and exit. The HCV-infected cells were co-stained with the LD marker (BODIPY 493/503), the

early endosome marker (early endosome antigen 1; EEA1), the late endosome marker (lysosome-associated membrane protein-1; Lamp-1), or the microtubule marker (β-tubulin). In the perinuclear region of cytoplasm, both the NS5A-Core and NS4B-Core complexes colocalized with the LDs and the early endosomes (Fig. 5E and 5F). In contrast, in the peripheral region, only the NS5A-Core complex, but not the NS4B-Core, colocalized with the late endosomes (Fig. 5G). Immunoelectron microscopy (immuno-EM) further showed that the late endosome/MVB contained NS5A, but not NS4B, the latter being mainly in the perinuclear regions (Fig. 5H). These results suggested strongly that NS5A-Core complexes, but not NS4B, are transported through early-to-late endosomes following virus assembly at LD.

Furthermore, NS5A and Core protein, but not NS4B, colocalized with the microtubules in the peripheral region of cytoplasm, especially at the microtubule end that is closest to the cell periphery (Fig. 6A). Finally, we characterized the relationship of NS5A-Core complexes with the plasma membrane. HCV-infected cells were co-stained with fluorescent (Alexa 647) WGA, anti-Core, and anti-NS5A or -NS4B Abs. As shown in Fig. 6B, NS5A and Core protein colocalized at the plasma membrane, particularly at the membrane curvature, which has been reported to be essential for virus exit [48]. Quantitative analysis showed that the number of anti-Core and anti-NS5A antibodies-labeled signals at the plasma membrane averaged 63 and 26 per cell, respectively, whereas that for anti-NS4B was less than 1. Interestingly, some signals containing both NS5A and Core (5 per cell on average) were also detected at the plasma membrane, whereas no NS4B-Core signals were found (Fig. 6C). Furthermore, immuno-EM showed that NS5A (Fig. 6D), Core protein (Fig.6E) and the Core-NS5A complex (Fig. 6F) localized mainly to patches or clusters on the plasma membrane. Taken together, these results again suggest that at least some of NS5A-Core complexes (or the assembled virions) are transported from LD through early-to-late endosomes to the plasma membrane via microtubules.

Identification of NS5A and exosomal proteins as low-density HCV virion-associated proteins

To confirm that NS5A is released from the plasma membrane as a component of some virion particles, we cultured HCV-infected Huh7.5 cells with dialyzed serum to reduce nonspecific binding of irrelevant proteins to virus particles. The culture supernatant was subject to sucrose gradient sedimentation, and the distribution of the viral RNA and infectivity of HCV were
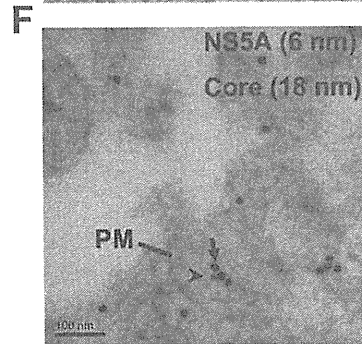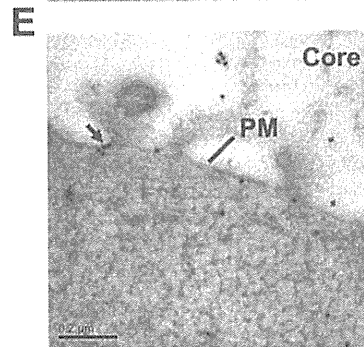
A NS5A/Core/tubulin/DAPI   Regions of cytoplasm

Perinuclear   Peripheral

NS4B/Core/tubulin/DAPI

B Core/NS5A/WGA/DAPI

Core/NS4B/WGA/DAPI

PM

D NS5A

PM

E Core

PM

F NS5A (6 nm)
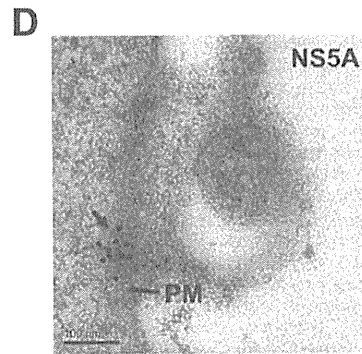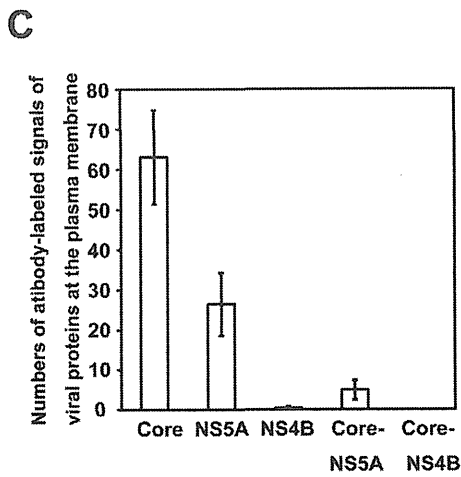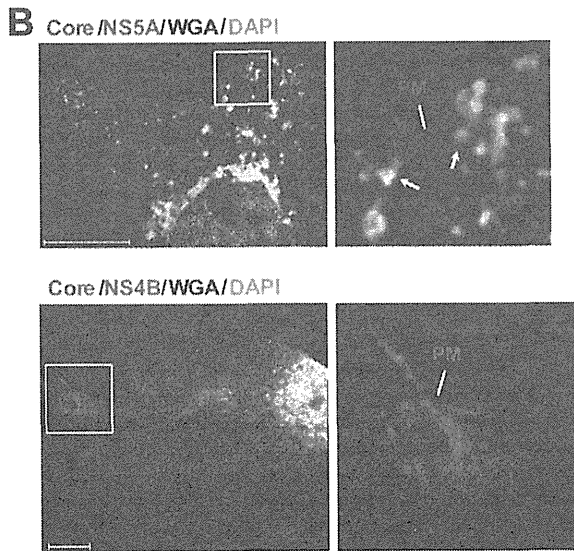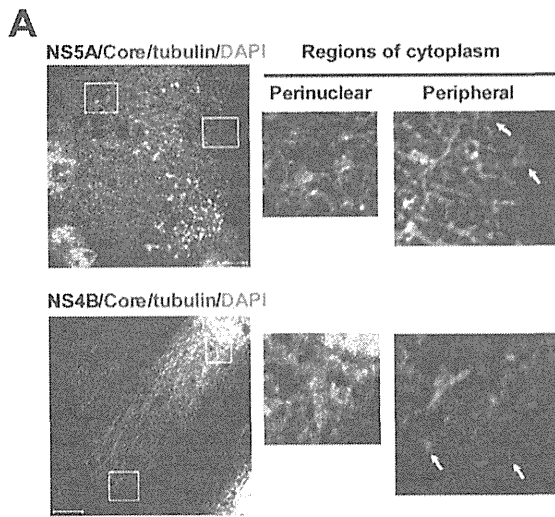Core (18 nm)

PM

C

−84−

Figure 6. Core-NS5A complexes are transported from perinuclear region to the plasma membrane via microtubules. The HCV-infected cells (at day 10 p.i.) were labeled with antibodies to Core protein (red) (A, B), NS5A (blue, A; green, B) (upper rows), NS4B (blue, A; green, B) (lower row) or tubulin (green) (A). Plasma membrane and nuclei were stained with WGA Alexa Fluor 647 conjugate (blue) (B) and DAPI (gray), respectively. The second and third panels in each row are magnified views, marked with a white box in the panel at the extreme left, of the perinuclear and the peripheral regions of cytoplasm, respectively (A). Colocalization of Core with NS5A or NS4B is depicted as magenta (A) or yellow (B). Colocalization of Core-NS5A or -NS4B protein complexes with microtubules (A) or plasma membrane (B) is depicted as white. The microtubule end (white arrow) is closest to the cell periphery (A). (B) At the right is an enlarged area, marked with a white box, from the merged image. Colocalization of NS5A with Core protein was observed in the membrane curvature (white arrow). PM, plasma membrane; Bars, 10 μm. (C) Quantitation of antibody-labeled signals of viral proteins at the plasma membrane. Images from 20 cells were counted manually using an original magnification of ×630 and followed by a quantitation analysis performed by an observer blinded to the experimental treatment. (D, E) NS5A and Core are localized in clusters or patches on the plasma membrane. In parallel, the HCV-infected cells were labeled with anti-NS5A (D) or anti-Core (E) antibodies. Bound antibodies were detected using anti-mouse secondary antibodies conjugated to 18-nm gold particles. Sections were visualized by EM. Arrows, gold-labeled NS5A (D) or Core protein (E). (F) Immuno-EM of Core-NS5A complex colocalized at the plasma membrane. The HCV-infected cells were co-labeled with antibodies against NS5A (6 nm) and Core (18 nm). Shown is a view of the plasma membrane. Arrowhead, gold-labeled NS5A. Arrow, gold-labeled Core. PM, plasma membrane; Bars, 100 nm (D, F) and 200 nm (E).
doi:10.1371/journal.pone.0099022.g006

determined. Two peaks, one from fractions 7–8, with density of 1.083 to 1.098 g/ml sucrose (low-density fractions; LDF), and another from fractions 11–13 with density of 1.145 to 1.178 g/ml sucrose (high-density fractions; HDF), were found to contain distinct HCV RNA signals (Fig. 7A). Fraction 12, at 1.162 g/ml sucrose, contains the largest amount of viral RNA, consistent with the previously reported density of free HCV virions [27,31]. Each fraction was further analyzed for its infectivity on naïve Huh7.5 cells. The results showed that both the LDF and HDF from culture supernatant contained infectivity (Fig. 7B), with HDF having approximately 153-fold higher specific infectivity. Thus, both the LDF and HDF are infectious, but LDF contained only 0.65% of the total infectivity; thus, the possibility that the apparent infectivity of LDF may have come from contaminations of HDF cannot be ruled out.

Further, we analyzed the various fractions for the possible presence of Core and NS5A. As shown in Fig. 7C, the HDF contained abundant Core protein, but no NS5A or NS4B. In contrast, the low-density fraction 7 (1.083 g/ml) contained NS5A in addition to Core protein, but no NS4B. Recent studies have revealed that HCV virion release requires late endosome (or multivesicular body; MVB) [10], the functional endosomal sorting complex required for transport (ESCRT) [46,47] and hepatocyte receptor tyrosine kinase substrate (Hrs) [45], all of which are involved in the biogenesis of MVB and exosome secretion. In addition, HCV particles are associated with circulating exosomes in hepatitis patients' serum [49]. We therefore investigated whether HCV virion release from cell membrane occurs through the exosome pathway. We probed each sucrose density fraction for the presence of two exosomal markers viz. CD81 and CD63. Interestingly, both CD81 and CD63 were detected in LDF (Fig. 7C), but not HDF, suggesting that the exosome is involved only in LDF virus release.

Since exosomes are derived from endosomes and are also secreted from normal cells to participate in a variety of cellular functions [50], we also analyzed the sucrose gradient fractions of extracellular medium obtained from naïve Huh7.5 cells and cells harboring an HCV subgenomic replicon. None of the fractions obtained from these cells contained HCV NS5A protein (data not shown), consistent with the previous report [34]. These data suggest that LDF contained HCV particles released through exosome-like structure, and contained NS5A.

The morphology and composition of virus particles in both the LDF and HDF were further characterized. The diameter of particles ranged from 105 to 132 nm (n = 60) and 52 to 86 nm (n = 90) in the low- and high-density pools, respectively (Fig. 7D and 7G). The size heterogeneity of HCV particles has been described previously [20,25,31]. Correspondingly, particles of ~130 nm and ~70 nm in diameter, probably representing the

low- and high-density virus particles, respectively, were observed in the extracellular space surrounding the HCV-infected cells (Fig. S1). After treatment with saponin (0.01%), which removed the viral envelope, the size of the particles was reduced to 35-41 nm for both the LDF and HDF viruses (Fig. 7E and 7F), consistent with its being the internal viral core [20,51].

Next, the purified virions were characterized for the presence of viral proteins and exosomal marker CD81 by immuno-EM. The particles in the low-density pool could be stained with anti-CD81 and -E2 MAbs, but not with a purified normal IgG or an anti-NS5A MAb (Fig. 7D, upper panels) or an anti-NS4B Ab (data not shown). In contrast, only E2 protein, but not CD81, was detected in the high-density pool (Fig. 7D, lower panels). The association of HCV envelope proteins with exosomes has previously been reported [49]. Following the treatment of virus samples with detergent (0.01% saponin), the virion core of both the low- and high-density pools was stained with anti-Core MAb (Fig. 7E). Interestingly, the virion core of LDF, but not the HDF, could be stained with anti-NS5A antibody, but neither normal IgG nor anti-NS4B antibody (Fig. 7E). In parallel, the saponin-treated virus of LDF could be stained with both Core and NS5A simultaneously (Fig. 7F). The specificity of staining was confirmed by staining under various treatment conditions (Fig. 7H). In all virus samples, normal IgG or anti-NS4B antibody yielded only background staining. In HDF, anti-CD81 and -NS5A antibodies also yielded very little staining with or without the saponin treatment. In contrast, in LDF, anti-CD81 (40%) and -E2 (25%) stained intact virus samples strongly, while anti-Core (70%) and -NS5A (40%) stained saponin-treated samples strongly.

The above results prompted us to further characterize the localization of the exosomal proteins relative to NS5A and Core protein on the plasma membrane. The results indicated that NS5A or Core protein colocalized with CD81 at the plasma membrane by immunofluorescence staining (Fig. 8A) and immuno-EM (Fig. 8B and 8C), but not NS4B. These results again suggest that some NS5A-containing HCV particles exit the cells via fusion of MVB with the plasma membrane. Taken together, these data suggest that a minor population of HCV virion exits cells via exosomes, as NS5A-containing, low-density particles, but the majority of virions do not contain NS5A and exit cells through an exosome-independent pathway.

Discussion

In this study, we found that in the presence of a microtubule-disrupting drug, both NS5A and Core proteins failed to be transported to the LD (Fig. 2), resulting in the accumulation of NS5A and Core protein in the ER (Fig. 3). In addition, NS5A and Core protein colocalized with microtubule throughout the entire
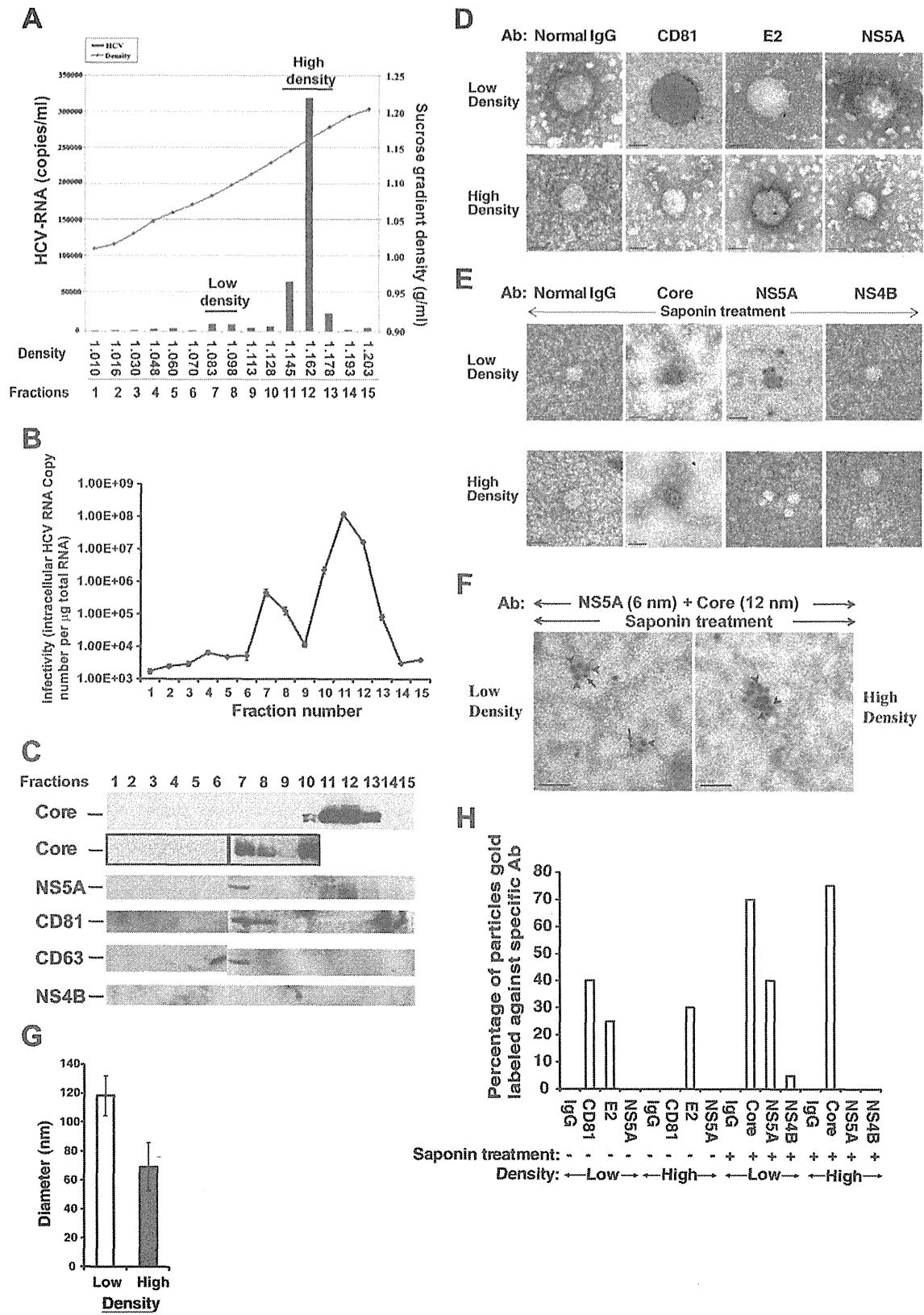
-86-

Figure 7. Association of NS5A and exosomal proteins with the low-density HCV particles. HCV virion populations were analyzed by sucrose density gradient ultracentrifugation. (A) Concentrated culture medium collected from HCV Jc1-infected cells was fractionated using a continuous 10–50% sucrose density gradient. HCV RNA levels were determined in each fraction. (B) Infectivity of each density gradient fraction. An aliquot of each fraction was used to infect naive Huh7.5 cells. Intracellular HCV RNA copy number per μg of total RNA was determined 3 days after infection by qRT-PCR. (C) Western blot analysis of each density gradient fraction, shown in panel A, by using antibodies indicated at the left. (D, E and F) Electron micrograph of the viral spherical structures shown by immunogold labeling. HCV particles were purified from two pooled fractions; the low-density particles (from fractions 7 to 8), and the high-density particles (from fractions 11 to 13), after dialysis and concentration. The virus samples were untreated (D) or treated with 0.01% saponin (E, F), as described in Materials and Methods. Grids were incubated with an untreated or saponin-treated purified HCV and then with antibodies against CD81, E2, or NS5A (D) or with antibodies against Core protein, NS5A or NS4B (E), respectively. Bound antibodies were detected using anti-mouse or -rabbit secondary antibodies conjugated to 12-nm gold particles. (F) Core-NS5A complex localized in the virion core of the low-density particles. Grids were incubated with a saponin-treated purified HCV and then co-labeled with antibodies against NS5A (6 nm) and Core (12 nm). To determine antibody specificity, primary antibodies were replaced with nonspecific normal mouse IgG. Bars, 50 nm. (G) The average diameter of the low- (n = 60) and high-density (n = 90) particles was obtained from the combined analysis of two independent viral preparations and error bars represent standard deviations of the mean. (H) Statistics were performed by counting HCV particles and immunogold labeled HCV particles from the combined analysis of two independent viral preparations. Relative proportion of HCV particles that were labeled with antibodies (n = 60).
doi:10.1371/journal.pone.0099022.g007

cytoplasm, mostly also associated with LDs (Fig. 1) and at the microtubule end near the plasma membrane (Fig. 6A). These results suggest that the intact microtubule network served as a transport highway for the movement of HCV NS5A (or viral RCs) and Core proteins from the ER towards the LD and plasma

membrane for virus assembly and exit. Additionally, it has been shown that the interaction between NS5A and Core protein on LDs plays an important role for virus assembly [18,19], and that Core protein induces redistribution of LD to the perinuclear region for virus assembly in a microtubule-dependent manner
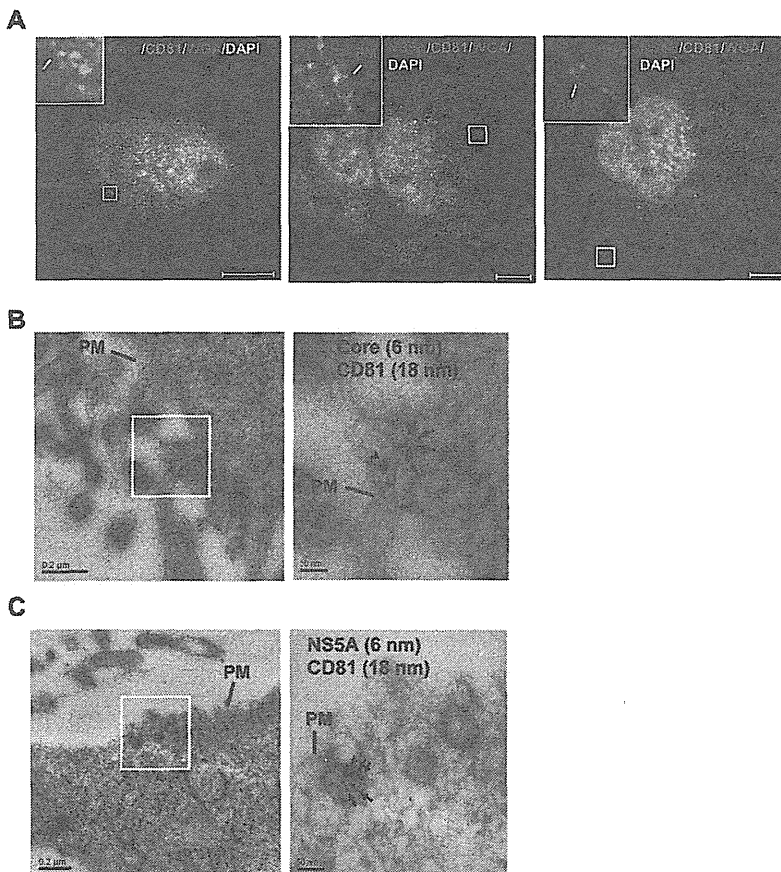
Figure 8. Colocalization of NS5A and Core protein with exosomal proteins at the plasma membrane. (A) The HCV-infected cells (at day 10 p.i.) were co-stained with anti-Core (red) (left panel) or -NS5A (red) (middle panel) or -NS4B (red) (right panel) and anti-CD81 (green). Plasma membrane and nuclei were stained with WGA Alexa Fluor 647 conjugate (blue) and DAPI (gray), respectively. Enlarged views of parts of every image (insets) are shown. PM, plasma membrane; Bars, 10 μm. (B, C) Immuno-EM of plasma membrane co-labeled with antibodies against Core (6 nm) (B) or NS5A (6 nm) (C) and CD81 (18 nm) are shown. Arrowheads, gold-labeled CD81. Arrows, gold-labeled Core and NS5A. Bars, 200 nm and 50 nm (B and C, left and right panels, respectively).
doi:10.1371/journal.pone.0099022.g008

−87−

[11]. These studies explain previous finding that the extracellular virus production was decreased by nocodazole [10].

By immunofluorescence staining and EM, we found that NS5A is closely associated with Core protein in almost every step of HCV life cycle, whereas NS4B is not involved in the late steps. However, only a small number (5 signals/cell) of the NS5A-Core complexes were detected at the plasma membrane of the cells, in contrast to Core protein alone (~63 signals/cell) (Fig. 6C). This finding may explain why the amount of HCV RNA in LDF (~1×10^4 copies/ml) was significantly lower than that of HDF (1.3×10^5 copies/ml) (Fig. 7A). We suggest that NS5A-containing, low-density HCV particles constitute a minor population of the released HCV virions. Nonetheless, this population was apparently infectious, though with slightly lower specific infectivity than the bulk of virus particles in HDF (Fig. 7B). The result is similar to a published report, which showed that less than 2% of all infectivity was in the low-density pool (density of <1.1g/ml) [20]. However, we cannot exclude the possibility that LDF with very weak infectivity may have come from virus contamination from HDF.

Notably, we demonstrated that low-density HCV particles utilize a host exosome biogenesis pathway for the production of NS5A-containing virions. The low-density HCV particles (density of 1.08 g/ml) were also found in hepatitis C patients' serum [26,52,53]. Most importantly, NS5A and exosomal markers coincided with Core protein in the low-density fractions (Fig. 7C), which also contained HCV RNA (Fig. 7A). NS5A-Core complexes (Fig. 7F) and exosomal markers (Fig. 7D) were detected in purified LDF virions. Correspondingly, exosomal markers and NS5A or Core protein were colocalized at the plasma membrane, where virus release occurs, as revealed by immunofluorescence staining and Immuno-EM (Fig. 8). Taken together, the results indicated that the low-density, NS5A-containing virions are released off the cell via exosomes, whereas the high-density particles exit the cell via some alternative mechanism not involving the exosomal pathway. Consistent with this hypothesis, HCV particles have been found to be associated with circulating exosomes in serum of HCV-infected patients [49]. Combined with our previous results [10] showing that HCV particles are transported from early to late endosomes/MVB, our current studies suggest that the NS5A-containing HCV particles most likely exit the cells via fusion of MVB to the plasma membrane. Exosomes have been demonstrated to facilitate the budding of human immunodeficiency virus (HIV) [54] and hepatitis A virus (HAV) [55]. Exosome have been known to play important roles in intercellular communications. In HIV and HAV infection, exosomes are required for trans-infection of CD4$^+$ T cells [56] and are likely to promote virus spread within the liver [55], respectively. Similarly, exosome-containing HCV virions might fuse to uninfected cell in a mechanism independent of viral envelope proteins and may contribute to HCV natural infection.

Interaction of NS5A with Core protein plays an important role in HCV particle production [19], but its mechanism of involvement in infectious virus production is still unclear. The association of viral NS proteins with viral genomic RNA and their incorporation into viral particles is common among RNA viruses, such as the NS2 of influenza virus [57], the V protein of simian

virus 5 [58], the NS3 of coronavirus [59], and the Vpx (viral protein X) of HIV-1 [60]. However, in contrast to our observation, Merz et al. [24] could not observe any NS5A in the virus preparation after affinity purification. The reason for this discrepancy may lie in the sensitivity of detection methods and the method of virus purification, as NS5A was detected only in a minor population of low-density particles in our study. It was also possible that the affinity tag used in the previous study [24] could not be detected in the low-density HCV particles.

Such virion-associated "nonstructural proteins" probably do not play structural roles in virus particles, but may participate in some yet unknown functions required at different steps of the viral life cycle. Recently, an amphipathic α-helical peptide (AH) containing the N-terminal 31 amino acids of NS5A was shown to induce swelling of the vesicles leading to vesicle lysis [61]; in addition, the infectivity of HCV particle was reduced when HCV virions were first treated with the AH peptide, causing the disruption of HCV envelope [62]. Taken together, the data presented here and elsewhere show that NS5A may induce fusion and lysis of lipid vesicles as well as virus particles during the virus entry step. Since NS5A is present inside the virus particles, it is likely that these membrane-altering functions of NS5A could function at a post-binding step, namely, after the virus envelope has been disrupted. Indeed, a postbinding fusion step within an acidic endosomal compartment is required for HCV entry [63]. This will be an interesting topic to study in the future.

In summary, our data demonstrated that a minor population of low-density HCV virions was released in the form of exosome from the infected cells, and that its virion core contains NS5A via close interaction with Core protein during intracellular transport. Our studies provide an additional target for designing new therapeutic approaches by possible use of exosome inhibitor to block the spread of HCV infection.

Supporting Information

Figure S1 The HCV-infected cells (at day 10 p.i.) were fixed and processed for EM. At the right is an enlarged area. The large-diameter (A, white arrows) and small-diameter (B, black arrows) HCV-like particles were released from plasma membrane. PM, plasma membrane; Bars, 500 nm (left panels) and 100 nm (right panels).
(TIF)

Acknowledgments

Author Contributions

Conceived and designed the experiments: CKL MML. Performed the experiments: CKL VS. Analyzed the data: CKL VS CHT MML. Contributed reagents/materials/analysis tools: KSJ MK MML. Wrote the paper: CKL MML.

References

1. Lohmann V, Koch JO, Bartenschlager R (1996) Processing pathways of the hepatitis C virus proteins. J Hepatol 24: 11–19.
2. Grakoui A, Wychowski C, Lin C, Feinstone SM, Rice CM (1993) Expression and identification of hepatitis C virus polyprotein cleavage products. J Virol 67: 1385–1395.
3. Blight KJ, Kolykhalov AA, Rice CM (2000) Efficient initiation of HCV RNA replication in cell culture. Science 290: 1972–1974.
4. Lohmann V, Korner F, Koch J, Herian U, Theilmann L, et al. (1999) Replication of subgenomic hepatitis C virus RNAs in a hepatoma cell line. Science 285: 110–113.
5. Egger D, Wolk B, Gosert R, Bianchi L, Blum HE, et al. (2002) Expression of hepatitis C virus proteins induces distinct membrane alterations including a candidate viral replication complex. J Virol 76: 5974–5984.

6. Gosert R, Egger D, Lohmann V, Bartenschlager R, Blum HE, et al. (2003) Identification of the hepatitis C virus RNA replication complex in Huh-7 cells harboring subgenomic replicons. J Virol 77: 5487–5492.
7. Lai CK, Jeng KS, Machida K, Lai MM (2008) Association of hepatitis C virus replication complexes with microtubules and actin filaments is dependent on the interaction of NS3 and NS5A. J Virol 82: 8838–8848.
8. Bost AG, Venable D, Liu L, Heinz BA (2003) Cytoskeletal requirements for hepatitis C virus (HCV) RNA synthesis in the HCV replicon cell culture system. J Virol 77: 4401–4408.
9. Roohvand F, Maillard P, Lavergne JP, Boulant S, Walic M, et al. (2009) Initiation of hepatitis C virus infection requires the dynamic microtubule network: role of the viral nucleocapsid protein. J Biol Chem 284: 13778–13791.
10. Lai CK, Jeng KS, Machida K, Lai MM (2010) Hepatitis C virus egress and release depend on endosomal trafficking of core protein. J Virol 84: 11590–11598.
11. Boulant S, Douglas MW, Moody L, Budkowska A, Targett-Adams P, et al. (2008) Hepatitis C virus core protein induces lipid droplet redistribution in a microtubule- and dynein-dependent manner. Traffic 9: 1268–1282.
12. Jones DM, McLauchlan J (2010) Hepatitis C virus: assembly and release of virus particles. J Biol Chem 285: 22733–22739.
13. Matsumoto M, Hwang SB, Jeng KS, Zhu N, Lai MM (1996) Homotypic interaction and multimerization of hepatitis C virus core protein. Virology 218: 43–51.
14. Shimoike T, Mimori S, Tani H, Matsuura Y, Miyamura T (1999) Interaction of hepatitis C virus core protein with viral sense RNA and suppression of its translation. J Virol 73: 9718–9725.
15. Miyanari Y, Atsuzawa K, Usuda N, Watashi K, Hishiki T, et al. (2007) The lipid droplet is an important organelle for hepatitis C virus production. Nat Cell Biol 9: 1089–1097.
16. Rouille Y, Helle F, Delgrange D, Roingeard P, Voisset C, et al. (2006) Subcellular localization of hepatitis C virus structural proteins in a cell culture system that efficiently replicates the virus. J Virol 80: 2832–2841.
17. Abid K, Pazienza V, de Gottardi A, Rubbia-Brandt L, Conne B, et al. (2005) An in vitro model of hepatitis C virus genotype 3a-associated triglycerides accumulation. J Hepatol 42: 744–751.
18. Appel N, Zayas M, Miller S, Krijnse-Locker J, Schaller T, et al. (2008) Essential role of domain III of nonstructural protein 5A for hepatitis C virus infectious particle assembly. PLoS Pathog 4: e1000035.
19. Masaki T, Suzuki R, Murakami K, Aizaki H, Ishii K, et al. (2008) Interaction of hepatitis C virus nonstructural protein 5A with core protein is critical for the production of infectious virus particles. J Virol 82: 7964–7976.
20. Gastaminza P, Dryden KA, Boyd B, Wood MR, Law M, et al. (2010) Ultrastructural and biophysical characterization of hepatitis C virus particles produced in cell culture. J Virol 84: 10999–11009.
21. Lindenbach BD, Evans MJ, Syder AJ, Wolk B, Tellinghuisen TL, et al. (2005) Complete replication of hepatitis C virus in cell culture. Science 309: 623–626.
22. Lindenbach BD, Meuleman P, Ploss A, Vanwolleghem T, Syder AJ, et al. (2006) Cell culture-grown hepatitis C virus is infectious in vivo and can be recultured in vitro. Proc Natl Acad Sci U S A 103: 3805–3809.
23. Grove J, Nielsen S, Zhong J, Bassendine MF, Drummer HE, et al. (2008) Identification of a residue in hepatitis C virus E2 glycoprotein that determines scavenger receptor BI and CD81 receptor dependency and sensitivity to neutralizing antibodies. J Virol 82: 12020–12029.
24. Merz A, Long G, Hiet MS, Brugger B, Chlanda P, et al. (2011) Biochemical and morphological properties of hepatitis C virus particles and determination of their lipidome. J Biol Chem 286: 3018–3032.
25. Andre P, Komurian-Pradel F, Deforges S, Perret M, Berland JL, et al. (2002) Characterization of low- and very-low-density hepatitis C virus RNA-containing particles. J Virol 76: 6919–6928.
26. Bradley D, McCaustland K, Krawczynski K, Spelbring J, Humphrey C, et al. (1991) Hepatitis C virus: buoyant density of the factor VIII-derived isolate in sucrose. J Med Virol 34: 206–208.
27. Kaito M, Watanabe S, Tsukiyama-Kohara K, Yamaguchi K, Kobayashi Y, et al. (1994) Hepatitis C virus particle detected by immunoelectron microscopic study. J Gen Virol 75 (Pt 7): 1755–1760.
28. Li X, Jeffers LJ, Shao L, Reddy KR, de Medina M, et al. (1995) Identification of hepatitis C virus by immunoelectron microscopy. J Viral Hepat 2: 227–234.
29. Prince AM, Huima-Byron T, Parker TS, Levine DM (1996) Visualization of hepatitis C virions and putative defective interfering particles isolated from low-density lipoproteins. J Viral Hepat 3: 11–17.
30. Wakita T, Pietschmann T, Kato T, Date T, Miyamoto M, et al. (2005) Production of infectious hepatitis C virus in tissue culture from a cloned viral genome. Nat Med 11: 791–796.
31. Heller T, Saito S, Auerbach J, Williams T, Moreen TR, et al. (2005) An in vitro model of hepatitis C virion production. Proc Natl Acad Sci U S A 102: 2579–2583.
32. Raposo G, Nijman HW, Stoorvogel W, Liejendekker R, Harding CV, et al. (1996) B lymphocytes secrete antigen-presenting vesicles. J Exp Med 183: 1161–1172.
33. Fevrier B, Raposo G (2004) Exosomes: endosomal-derived vesicles shipping extracellular messages. Curr Opin Cell Biol 16: 415–421.
34. Dreux M, Garaigorta U, Boyd B, Decembre E, Chung J, et al. (2012) Short-range exosomal transfer of viral RNA from infected cells to plasmacytoid dendritic cells triggers innate immunity. Cell Host Microbe 12: 558–570.
35. Blight KJ, McKeating JA, Rice CM (2002) Highly permissive cell lines for subgenomic and genomic hepatitis C virus RNA replication. J Virol 76: 13001–13014.
36. Parent R, Qu X, Petit MA, Beretta L (2009) The heat shock cognate protein 70 is associated with hepatitis C virus particles and modulates virus infectivity. Hepatology 49: 1798–1809.
37. Lai CK, Jeng KS, Machida K, Cheng YS, Lai MM (2008) Hepatitis C virus NS3/4A protein interacts with ATM, impairs DNA repair and enhances sensitivity to ionizing radiation. Virology 370: 295–309.
38. Pietschmann T, Kaul A, Koutsoudakis G, Shavinskaya A, Kallis S, et al. (2006) Construction and characterization of infectious intragenotypic and intergenotypic hepatitis C virus chimeras. Proc Natl Acad Sci U S A 103: 7408–7413.
39. Cai Z, Zhang C, Chang KS, Jiang J, Ahn BC, et al. (2005) Robust production of infectious hepatitis C virus (HCV) from stably HCV cDNA-transfected human hepatoma cells. J Virol 79: 13963–13973.
40. Saxena V, Lai CK, Chao TC, Jeng KS, Lai MM (2012) Annexin A2 is involved in the formation of hepatitis C virus replication complex on the lipid raft. J Virol 86: 4139–4150.
41. Listenberger LL, Brown DA (2007) Fluorescent detection of lipid droplets and associated proteins. Curr Protoc Cell Biol Chapter 24: Unit 24.22.
42. Nelson HB, Tang H (2006) Effect of cell growth on hepatitis C virus (HCV) replication and a mechanism of cell confluence-based inhibition of HCV RNA and protein expression. J Virol 80: 1181–1190.
43. Shi ST, Lee KJ, Aizaki H, Hwang SB, Lai MM (2003) Hepatitis C virus RNA replication occurs on a detergent-resistant membrane that cofractionates with caveolin-2. J Virol 77: 4160–4168.
44. Coller KE, Heaton NS, Berger KL, Cooper JD, Saunders JL, et al. (2012) Molecular determinants and dynamics of hepatitis C virus secretion. PLoS Pathog 8: e1002466.
45. Tamai K, Shiina M, Tanaka N, Nakano T, Yamamoto A, et al. (2012) Regulation of hepatitis C virus secretion by the Hrs-dependent exosomal pathway. Virology 422: 377–385.
46. Ariumi Y, Kuroki M, Maki M, Ikeda M, Dansako H, et al. (2011) The ESCRT system is required for hepatitis C virus production. PLoS One 6: e14517.
47. Corless L, Crump CM, Griffin SD, Harris M (2010) Vps4 and the ESCRT-III complex are required for the release of infectious hepatitis C virus particles. J Gen Virol 91: 362–372.
48. Falanga A, Cantisani M, Pedone C, Galdiero S (2009) Membrane fusion and fission: enveloped viruses. Protein Pept Lett 16: 751–759.
49. Masciopinto F, Giovani C, Campagnoli S, Galli-Stampino L, Colombatto P, et al. (2004) Association of hepatitis C virus envelope proteins with exosomes. Eur J Immunol 34: 2834–2842.
50. Meckes DG Jr, Raab-Traub N (2011) Microvesicles and viral infection. J Virol 85: 12844–12854.
51. Ishida S, Kaito M, Kohara M, Tsukiyama-Kohora K, Fujita N, et al. (2001) Hepatitis C virus core particle detected by immunoelectron microscopy and optical rotation technique. Hepatol Res 20: 335–347.
52. Kanto T, Hayashi N, Takehara T, Hagiwara H, Mita E, et al. (1994) Buoyant density of hepatitis C virus recovered from infected hosts: two different features in sucrose equilibrium density-gradient centrifugation related to degree of liver inflammation. Hepatology 19: 296–302.
53. Miyamoto H, Okamoto H, Sato K, Tanaka T, Mishiro S (1992) Extraordinarily low density of hepatitis C virus estimated by sucrose density gradient centrifugation and the polymerase chain reaction. J Gen Virol 73 (Pt 3): 715–718.
54. Sette P, Mu R, Dussupt V, Jiang J, Snyder G, et al. (2011) The Phe105 loop of Alix Bro1 domain plays a key role in HIV-1 release. Structure 19: 1485–1495.
55. Feng Z, Hensley L, McKnight KL, Hu F, Madden V, et al. (2013) A pathogenic picornavirus acquires an envelope by hijacking cellular membranes. Nature 496: 367–371.
56. Izquierdo-Useros N, Naranjo-Gomez M, Erkizia I, Puertas MC, Borras FE, et al. (2010) HIV and mature dendritic cells: Trojan exosomes riding the Trojan horse? PLoS Pathog 6: e1000740.
57. Richardson JC, Akkina RK (1991) NS2 protein of influenza virus is found in purified virus and phosphorylated in infected cells. Arch Virol 116: 69–80.
58. Paterson RG, Leser GP, Shaughnessy MA, Lamb RA (1995) The paramyxovirus SV5 V protein binds two atoms of zinc and is a structural component of virions. Virology 208: 121–131.
59. Neuman BW, Joseph JS, Saikatendu KS, Serrano P, Chatterjee A, et al. (2008) Proteomics analysis unravels the functional repertoire of coronavirus nonstructural protein 3. J Virol 82: 5279–5294.
60. Wu X, Conway JA, Kim J, Kappes JC (1994) Localization of the Vpx packaging signal within the C terminus of the human immunodeficiency virus type 2 Gag precursor protein. J Virol 68: 6161–6169.
61. Cho NJ, Wang G, Edvardsson M, Glenn JS, Hook F, et al. (2009) Alpha-helical peptide-induced vesicle rupture revealing new insight into the vesicle fusion process as monitored in situ by quartz crystal microbalance-dissipation and reflectometry. Anal Chem 81: 4752–4761.
62. Cho NJ, Dvory-Sobol H, Xiong A, Cho SJ, Frank CW, et al. (2009) Mechanism of an amphipathic alpha-helical peptide's antiviral activity involves size-dependent virus particle lysis. ACS Chem Biol 4: 1061–1067.
63. Blanchard E, Belouzard S, Goueslain L, Wakita T, Dubuisson J, et al. (2006) Hepatitis C virus entry depends on clathrin-mediated endocytosis. J Virol 80: 6964–6972.

—89—

Suppression of hepatitis C virus replication by cyclin-dependent kinase inhibitors

CrossMark

Tsubasa Munakata [a,b,*], Makoto Inada [b], Yuko Tokunaga [a], Takaji Wakita [c], Michinori Kohara [a], Akio Nomoto [b,d]

[a] Department of Microbiology and Cell Biology, Tokyo Metropolitan Institute of Medical Science, 2-1-6 Kamikitazawa, Setagaya-ku, Tokyo 156-8506, Japan
[b] Department of Microbiology, Graduate School of Medicine, The University of Tokyo, 7-3-1 Hongo, Bunkyo-ku, Tokyo 113-0033, Japan
[c] Department of Virology II, National Institute of Infectious Diseases, 1-23-1 Toyama, Shinjuku-ku, Tokyo 162-8640, Japan
[d] Institute of Microbial Chemistry, 3-14-23 Kamiohsaki, Shinagawa-ku, Tokyo 141-0021, Japan

ARTICLE INFO

ABSTRACT

Hepatitis C virus (HCV) is a causative agent of chronic hepatitis. Although the standard therapy for HCV-infected patients consists of pegylated interferon plus ribavirin, this treatment is associated with serious side effects and high costs, and fails in some patients infected with specific HCV genotypes. To address this problem, we are developing small-molecule inhibitors of cyclin-dependent kinases (CDKs) as novel anti-HCV drug candidates. Previous data showed that HCV replication is inhibited by retinoblastoma protein, which is itself inactivated by CDK-mediated phosphorylation. Here, we report that CDK inhibitors suppress HCV replication *in vitro* and *in vivo*, and that CDK4 is required for efficient HCV replication. These findings shed light on the development of novel anti-HCV drugs that target host factors.

© 2014 Elsevier B.V. All rights reserved.

1. Introduction

Hepatitis C virus (HCV) is a causative agent of chronic hepatitis, and persistent HCV infection is a major risk factor for the development of a range of liver diseases, including cirrhosis and hepatocellular carcinoma (HCC). As an estimated 170 million people worldwide are infected with HCV, this virus is an increasing concern for global public health (De Francesco and Migliaccio, 2005). HCV is classified into 6 major genotypes (designated 1–6) and several subtypes (designated a, b, c, etc.) (Simmonds et al., 2005). Types 1a and 1b are the most common, accounting for about 60% of global infections. Currently, the standard therapy for HCV-infected patients consists of treatment with pegylated interferon (PEG-IFN) plus ribavirin (Feld and Hoofnagle, 2005). This combination therapy has been quite successful in patients with HCV genotype 2 or 3 infections, leading to sustained virologic response (SVR) in more than 80% of patients treated (Pawlotsky, 2009). However, in patients infected with HCV genotype 1 or 4, only about 50% of treated individuals achieve SVR (Keeffe, 2007). Furthermore, treatment is often associated with serious side effects and high costs.

* Corresponding author at: Department of Microbiology and Cell Biology, Tokyo Metropolitan Institute of Medical Science, 2-1-6 Kamikitazawa, Setagaya-ku, Tokyo 156-8506, Japan. Tel.: +81 3 5316 3122; fax: +81 3 5316 3137.
E-mail address: munakata-tb@igakuken.or.jp (T. Munakata).

HCV is an enveloped virus with a positive-strand RNA genome. The 9.6-kb HCV genome encodes a single polyprotein processed by both cellular and viral proteases into at least 10 distinct structural (core, E1, E2, and p7) and nonstructural (2, 3, 4A, 4B, 5A, and 5B) proteins. Among these proteins, essential viral enzymes serve as potential candidates for targeting by antiviral therapy. Specifically, the NS3/4A serine protease and NS5B RNA polymerase have been the most popular targets (Waters and Nelson, 2006). A number of competitive inhibitors of NS3, as well as nucleoside and non-nucleoside inhibitors of NS5B, are being developed, although emergence of resistance to inhibitors has been observed *in vivo* and *in vitro* (Sarrazin et al., 2007). For instance, a single mutation is sufficient to confer resistance to a viral protease inhibitor, BILN 2061 (Lamarre et al., 2003; Lin et al., 2005). Very recently, the standard of care for treating chronic HCV infection has changed to a triple therapy of PEG-IFN, ribavirin and an HCV protease inhibitor such as telaprevir, boceprevir or vaniprevir (Macartney et al., 2014; Manns et al., 2012). However, emergence of resistance-associated variants after failed triple therapy remains a matter of concern, and severe side-effects such as anemia limit the choice of patients (Barnard et al., 2013; Poordad et al., 2013), suggesting that a novel approach is necessary to treat HCV infection.

Host mechanisms that regulate cell-cycle progression and cellular proliferation are disrupted in HCC associated with HCV

(Mayhew et al., 2007; Reed et al., 2010). Among cell-cycle regulators, retinoblastoma protein (Rb) plays a major role in controlling the G1- to S-phase transition and mitotic checkpoints through a repressive effect on E2F transcription factors (Chellappan et al., 1991; Chen et al., 2009). Rb functions as a tumor suppressor, and is targeted by oncoproteins expressed by DNA tumor viruses (Khidr and Chen, 2006; Knudson, 1971). In previous studies, we found that the NS5B polymerase forms a complex with Rb, targeting Rb for degradation (Munakata et al., 2007, 2005). This interaction leads to the activation of E2F-responsive promoters, and promotes progression of the cell cycle from G1- to S-phase in cells expressing NS5B. This interaction also inhibits NS5B polymerase activity, as Rb binds near the NS5B polymerase catalytic site. Given that the S phase facilitates HCV replication and translation, Rb thus is a negative regulator of HCV replication by two mechanisms (Honda et al., 2000; Scholle et al., 2004).

In addition to degradation, Rb can be inactivated by phosphorylation (Buchkovich et al., 1989). Cyclin-dependent kinases (CDKs) phosphorylate Rb at multiple sites to suppress the repressive function of Rb (Knudsen and Wang, 1996). In quiescent cells or cells in early G1, Rb binds to the E2F transcription factors and blocks the E2F transactivation domains, recruiting transcriptional co-repressors and resulting in the repression of E2F-responsive promoters (Chen et al., 2009). Under normal conditions, initiation or progression through the cell cycle requires growth signals that lead to the sequential activation of the CDK-cyclin complexes CDK4/6-cyclin D and CDK2-cyclin E, leading in turn to hyperphosphorylation of Rb and the release of active E2F (Simanis and Nurse, 1986; Uhlmann et al., 2011). In the present study, we used small-molecule CDK inhibitors to activate Rb (Krystof and Uldrijan, 2010; Whittaker et al., 2004). We found that CDK inhibitors suppress HCV replication *in vitro* and *in vivo*, and that CDK4 is required for efficient HCV replication. These findings shed light on the development of novel anti-HCV drugs that target host factors.

2. Materials and methods

2.1. Cells

Human hepatoma cells HuH-7 and its derivatives, including Huh7.5.1, were grown in Dulbecco modified Eagle medium (Invitrogen, Carlsbad, CA; GlutaMax grade) supplemented with 10% heat-inactivated fetal bovine serum, 100 U/ml penicillin G, and 100 μg/ml streptomycin, at 37 °C in a humidified atmosphere with 5% CO_2. The 2–3 cells were a HuH-7-derived cell line containing autonomously replicating, genome-length, dicistronic, selectable HCV RNAs that were derived from the genotype-1b HCV-N strain; the 2–3 cell line was cultured as above, with addition of 300 μg/ml G418 (Ikeda et al., 2002). Y19 and R6FLR-N were HuH-7-derived cell lines containing autonomously replicating, subgenomic, dicistronic, selectable HCV RNAs derived from genotype-2a JFH-1 and genotype-1b HCR6 and HCV-N strains, respectively; these cell lines were cultured as above, with the addition of 500 μg/ml G418. The cognate cell lines, interferon-cured progeny cell lines 2-3c and Y19c, were generated from the respective parent lines and were maintained as described previously (Ikeda et al., 2002), and contained no detectable HCV RNA by RT-PCR assay.

2.2. Viruses

Cell culture-infectious genotype-2a JFH-1 viruses were harvested from the culture medium supernatant of RNA-transfected HuH-7 cells, and stored at −80 °C until use. Huh7.5.1 cells were infected with JFH-1 virus as described previously (Munakata et al., 2007; Wakita et al., 2005), and HCV RNA titers of the infected cells were measured by real-time RT-PCR using a Light Cycler (Roche, Indianapolis, IN). Briefly, one microgram of RNA was reverse-transcribed and amplified using RNA Master Hybridization Probes Kit (Roche) with JFH-1 sense 62–81 (5′-TTC ACG CAG AAA GCG CCT AG-3′) and antisense 311–293 (5′-ACT CGC AAG CGC CCT ATC A-3′) primers, and was detected with LC179-207 (5′-GGA AGA CTG GGT CCT TTC TTG GAT AAA CC-3′-FITC) and LC209-233 (LC-Red-5′-ACT CTA TGC CCG GCC ATT TGG GCG T-3′) probes. Testing revealed that Huh7.5.1 + JFH-1 cells harbored approximately 1×10^7 copies of HCV genome per microgram of RNA.

2.3. CDK inhibitors

Roscovitine, CDK4 inhibitor, CDK2 inhibitor III, fascaplysin, aminopurvalanol A, and indirubin-3′-monoxime-5-sulfonic acid were purchased from Merck Chemicals (Philadelphia, PA); each was prepared as a solution in dimethyl sulfoxide (DMSO). Roscovitine was also purchased from ALEXIS Biochemicals (Farmingdale, NY). Detailed features of each inhibitor including IC50 for a target CDK are shown in Table 1, based on the manufacturer's information (McClue et al., 2002; Meijer et al., 1997).

For treatment of the replicon-carrying and HCV-infected cells, cells were seeded into 6-well plates and grown to 50% confluence. Inhibitors then were added to the culture medium at the indicated concentrations and were incubated for 24–48 h. Cell extracts were then processed to isolate protein (for immunoblots) or total RNA (for real-time RT-PCR).

2.4. Plasmids

CDK4 expression vector, pCMV6XL5-hCDK4, was purchased from Origene. The cDNA encoding cyclin D1 was cloned from a cDNA library of HuH-7 cells, and was subcloned into pcDNA3.1-zeo(+) (Invitrogen) to construct the *cyclin D1* expression vector, pcDNA3.1zeo(+)-hCyclinD1. For over-production of CDK4 or cyclin D1, Huh7.5.1 + JFH-1 cells were seeded into 6-well plates 24 h before transfection and grown to 50% confluence. At the time of transfection, culture medium was replaced with fresh medium without antibiotics. Cells then were transiently transfected with one of the expression plasmids using FuGENE 6 reagents (Roche). Protein extracts were prepared for immunoblots at 48 h after transfection.

2.5. RNA interference

For knockdown of cyclin D1, CDK2, CDK4, CDK6, and MDM2, siGENOME SMART pool siRNAs were purchased from Dharmacon (Pittsburgh, PA). For knockdown of Rb, Stealth RNAi siRNA was purchased from Invitrogen. As negative controls, non-targeting siRNAs and those against green fluorescent protein (GFP) were used. Further analysis of CDK4 knockdown was performed using the four individual siRNA molecules that are normally combined in the CDK4 SMART pool. Transfection with siRNAs was carried out using Lipofectamine 2000 (Invitrogen) as described previously (Munakata et al., 2007).

2.6. Luciferase assays

HCV replicon cells were seeded in 96-well plates at a density of 4×10^3 cells/well. After 24-h incubation, inhibitors were added to the growth medium, and after an additional 72-h incubation, luciferase assays were performed using the Bright-Glo luciferase assay kit (Promega, Madison, WI) according to the manufacturer's instructions. At the same time, cell viability was measured by WST-8 assay (Cell Counting Kit-8; Dojindo, Kumamoto, Japan) according to the manufacturer's instructions.

Table 1
Inhibitors of cyclin-dependent kinases (CDKs).

Inhibitor	Chemical name	Target CDK (in vitro IC50)	Mw
A	Roscovitine	CDK1 (650 nM),CDK2 (100 nM),CDK5 (200 nM)	354.5
B	CDK4 inhibitor	CDK1 (2.1 μM), CDK2 (520 nM), CDK4 (76 nM)	404.2
C	CDK2 inhibitor III	CDK1 (4.2 μM), CDK2 (500 nM), CDK4 (215 μM)	400.5
D	Fascaplysin	CDK4 (350 nM), CDK6 (3.4 μM)	306.8
E	Aminopurvalanol A	CDK1 (33 nM), CDK2 (28 nM), CDK5 (20 nM)	403.9
F	Indirubin-3'-monoxime-5-sulfonic acid	CDK1 (5 nM), CDK5 (7 nM)	357.3

Mw, molecular weight.

2.7. Immunoblots

Cell extracts were prepared in chilled lysis buffer (20 mM Tris–HCl [pH 7.5], 150 mM NaCl, 10 mM Na_2EDTA, 1% [v/v] Nonidet P-40, 10% [v/v] glycerol, and 2 mM dithiothreitol) supplemented with 1 mM phenylmethylsulfonyl fluoride and 2 μg/ml aprotinin. Sodium dodecyl sulfate polyacrylamide gel electrophoresis (SDS–PAGE) and subsequent immunoblotting were performed as described previously (Munakata et al., 2005), using mouse monoclonal antibodies against actin (C4; Chemicon, Billerica, MA), CDK4 (DCS-35; Santa Cruz Biotechnology, Santa Cruz, CA), cyclin D1 (DCS-6; Santa Cruz Biotechnology), HCV core (C7-50; Affinity BioReagents, Rockford, IL, USA), HCV NS3 (1828; ViroStat, Portland, ME, USA), HCV NS5A (#950328; Biken, Osaka, Japan), and Rb (G3-245; BD Biosciences, San Diego, CA), and rabbit polyclonal antibodies against BubR1 (A300-995A; Bethyl Laboratories, Montgomery, TX), CDK2 (M2; Santa Cruz Biotechnology), CDK6 (C-21; Santa Cruz Biotechnology), phospho-Rb Ser780 (#9307; Cell Signaling Technology, Danvers, MA) and HCV NS5B (ab35586; Abcam, Cambridge, MA).

2.8. Chimeric mice

Chimeric mice harboring a functional human liver cell xenograft were purchased from PhoenixBio (Hiroshima, Japan). Six weeks after human hepatocyte transplantation, we intravenously injected each mouse with an HCV-infected patient's serum containing 10^6 copies of HCV genotype 1b (HCR6; Accession No. AY045702) (Nakagawa et al., 2007). Protocols for the animal experiments were approved by the Ethics Committee of Tokyo Metropolitan Institute of Medical Science. Animals received humane care according to the guidelines of the National Institutes of Health. The HCV-infected patient who provided the serum provided written informed consent before blood sampling.

The 14-day drug administration was performed as follows. Roscovitine-treated mice received intravenous once-daily (day 0–day 13) injections of 25 or 50 mg/kg roscovitine. IFN-treated mice received subcutaneous twice-weekly (days 0, 3, 7, and 10) injections of 30 μg/kg PEG-IFNα-2a (Chugai, Tokyo, Japan). This IFN dose, administered approximately every 3 days, represented a 10-fold excess when compared to the regimen used once daily in clinical treatment. For all animals (mono- or combined therapy), blood was sampled on days −1, 1, 3, 7, 10, and 14.

For quantification of HCV RNA, total RNA was purified from 1 μl of serum from each mouse by the acid guanidinium–phenol–chloroform method, and HCV RNA was quantified by real-time RT-PCR as described previously (Nakagawa et al., 2007; Takeuchi et al., 1999). For end-point analysis, total RNA was prepared from the liver tissue of chimeric mice, and HCV RNA was quantified as above. RNA analysis of human actin, CDK2, CDK4, CDK6, and MDA5 was performed using TaqMan Gene Expression Assays (Applied Biosystems, Carlsbad, CA). Immunoblots of CDK proteins were performed as described above, using total protein lysates prepared by Tissue Lyser (Qiagen, Valencia, CA).

Human serum albumin in the blood of chimeric mice was measured using the Alb-II kit (Eiken Chemical, Tokyo, Japan) according to the manufacturer's instructions. Serum alanine aminotransferase (ALT) levels were measured using a Transaminase-CII Test A kit (Wako Pure Chemical Industries, Osaka, Japan).

2.9. Statistical analysis

Analyses were performed by two-tailed Student's t test using Excel 2003 (Microsoft, Redmond, WA). Mean and standard deviations were derived from at least three separate experiments. P values of <0.05 were considered statistically significant.

3. Results

3.1. CDK inhibitors suppress HCV replication

Our preliminary experiments employed three distinct HuH-7-derived human hepatoma cell lines. Cells of this background are known to support the autonomous replication of dicistronic HCV RNA replicons. The first of these cell lines (called R6FLR-N) contained a subgenomic replicon of the HCR6 and HCV-N strain of genotype 1b; this replicon produced only the NS3-NS5B region of the HCV polyprotein (Nakagawa et al., 2007). This cell line also expressed firefly luciferase, which enabled us to quantify replicon activity by measuring luciferase activity. The second cell line (called 2-3) contained replicating genome-length RNA that produced all of the proteins of HCV-N strain (Ikeda et al., 2002). The third cell line (called 2-3c) served as a control, and consisted of a cognate cell line that did not contain any HCV RNA.

In order to determine the effect(s) of CDK inhibition, we initially tested two CDK inhibitors (A and B; Table 1) in these HuH-7-derived cells, and examined HCV replication in the treated cells. As shown in Fig. 1a, CDK inhibitors A and B were able to suppress HCV replication in R6FLR-N replicon cells without affecting cell viability. Moreover, inhibitors A and B reduced the amount of HCV NS5B polymerase as well as that of phosphorylated Rb (Fig. 1b). There were no apparent changes in the amount of total Rb. For both A and B, the 50% effective concentrations (EC_{50}s) for suppression of HCV replication were submicromolar, and other CDK inhibitors, except F, were also able to suppress HCV replication (Supplementary Fig. 1). However, in 2–3 replicon cells, inhibitor B, but not A, suppressed HCV replication, as shown by the immunoblots of HCV NS5A and NS5B proteins (Fig. 1c). Although the effective dose of inhibitor B was higher in 2–3 than in R6FLR-N, this CDK inhibitor suppressed the replication of HCV of genotype 1b in vitro.

Next, we examined whether CDK inhibition suppressed the replication of HCV of other genotypes. For this purpose, we used a cell line (called Y19) that contained a subgenomic replicon of the JFH-1 strain of HCV genotype 2a, and a cognate cell line (called Y19c) that did not contain any HCV RNA (Kato et al., 2003), and assessed viral replication by real-time reverse transcription polymerase chain reaction (RT-PCR). Of the six CDK inhibitors tested (A–F; Table 1),
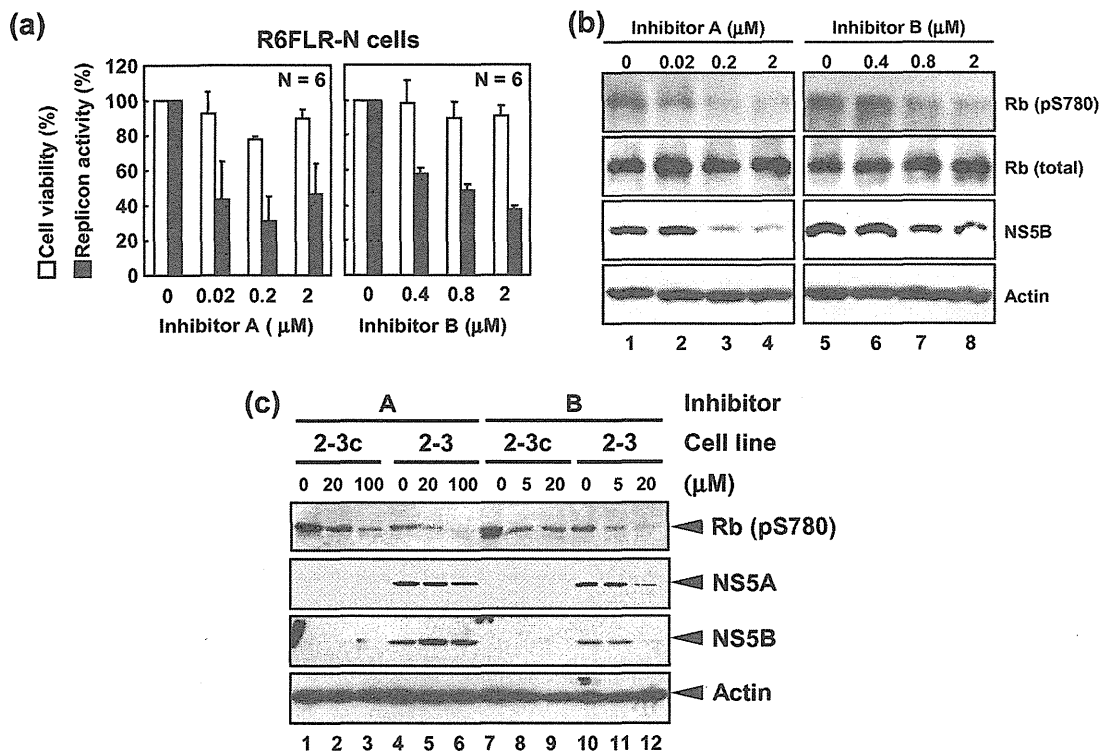
Fig. 1. CDK inhibitors suppress replication of HCV genotype 1b replicon. (a) Inhibition of HCV replicon activity in R6FLR-N cells. After addition of CDK inhibitor, HCV replication was measured by luciferase assay, and cell viability was measured by water-soluble tetrazolium (WST) salts assay. Data represent means ± SD from six experiments. (b) Reduction of HCV NS5B protein in R6FLR-N cells. After addition of CDK inhibitor, total protein was isolated and subjected to immunoblot analysis for HCV NS5B, Rb phosphorylated at Ser780 (pS780; confirmation of CDK inhibition), total Rb, and actin (loading control). CDK inhibitors decreased the amount of phosphorylated Rb in a dose-dependent manner. (c) Inhibition of HCV replicon activity of 2–3 cells. After addition of CDK inhibitor, total protein was isolated and subjected to immunoblot analysis for HCV NS5A, HCV NS5B, Rb phosphorylated at Ser780, and actin. As expected, 2-3c cells did not produce HCV proteins.

five (A, B, C, D, and E) were found to reduce the amount of HCV replicon RNA (Fig. 2a), without affecting cell viability (Supplementary Fig. 1b). We also found that these five inhibitors reduced the amounts of HCV NS5B and phosphorylated Rb proteins, as compared to controls (Fig. 2b). Specifically, inhibitors A, B, and E decreased HCV RNA and protein in a dose-dependent manner. Thus, CDK inhibitors suppressed the replication of genotype-2a HCV in vitro.

3.2. CDK inhibitors suppress HCV infection

The preceding experiments demonstrated the effects of CDK inhibitors on HCV replication in three distinct replicon cell lines. To address the effects of CDK inhibition on HCV infection, we employed a model of HCV infection in cultured hepatocytes. Specifically, we used the Huh7.5.1 + JFH-1 cell line, which corresponds to HuH-7-derived cells (designated Huh7.5.1) that have been infected in vitro with the JFH-1 strain of HCV (Wakita et al., 2005). HCV infection and reproduction was assayed using RT-PCR detection of HCV RNA genome levels. We found that CDK inhibitors B and E provided dose-dependent reductions in the levels of viral RNA in HCV-infected cells (Fig. 3a), demonstrating the suppression of HCV infection by CDK inhibition. Our data indicated that inhibitor B was the most effective of the 6 inhibitors tested. Inhibitor B was reported to selectively target CDK4 (Table 1) (Matsushime et al., 1992). Therefore, we hypothesized that CDK4 is a positive regulator of HCV replication in infected hepatocytes (Fig. 3b; Section 4).

In order to further demonstrate our hypothesis, we examined whether depletion of Rb, a downstream target of CDK4, rescued

suppression of HCV replication by inhibitor B. For this purpose, we first knocked down endogenous Rb using small interfering RNA (siRNA) transfection, and performed HCV replication inhibition assays (Fig. 3c). We found that the inhibitor B-dependent suppression of HCV replication was significantly attenuated by Rb knockdown (Fig. 3d and e). These data clearly indicate that CDK4 affects HCV replication through Rb.

3.3. CDK4 is a host factor required for HCV replication

In order to investigate whether CDK4 is actually required for HCV replication, we first performed RNA interference (RNAi) for knockdown of CDK4 in Y19 replicon cells. Immunoblot analysis demonstrated that knockdown of CDK4 reduced the amounts of CDK4 protein, as well as those of phosphorylated Rb and HCV NS5B proteins, as was the case with CDK inhibitors (Fig. 4a). To further examine whether CDK4 and/or its partner cyclin D are required for the HCV life cycle, we again used RNAi to perform knockdown of CDK4 and cyclin D1 in Huh7.5.1 + JFH-1 cells. Although cyclin D consists of D1, D2, and D3 sub-types, D2 and D3 are not normally produced in the liver, while cyclin D1 is induced in hepatic tumor cells (Musgrove et al., 2011; Teramoto et al., 1999). We therefore focused on cyclin D1 in our analysis. Following transfection with siRNAs that targeted the mRNAs encoding CDK4 or cyclin D1, we used immunoblotting to determine the levels of CDK4, cyclin D1, and HCV core protein. As shown in Fig. 4b, RNAi against CDK4 impaired the production of CDK4 protein and reduced levels of HCV core protein; RNAi against cyclin D1 reduced cyclin D1 production, but did not decrease HCV core protein levels. To demonstrate the specificity of CDK4 knockdown, we transfected

(a) Y19 replicon cells (N = 3)

Replicon RNA levels (Fold change)

Inhibitor	-	A	A	B	B	C	D	E	E	F
(µM)		50	100	5	10	20	1	10	20	50

(b) Y19c

| | - | A | A | B | B | C | D | E | E | F | Inhibitor |
| | | 50 | 100 | 5 | 10 | 20 | 1 | 10 | 20 | 50 | (µM) |

Rb (pS780)
Rb (total)
NS5B
Actin

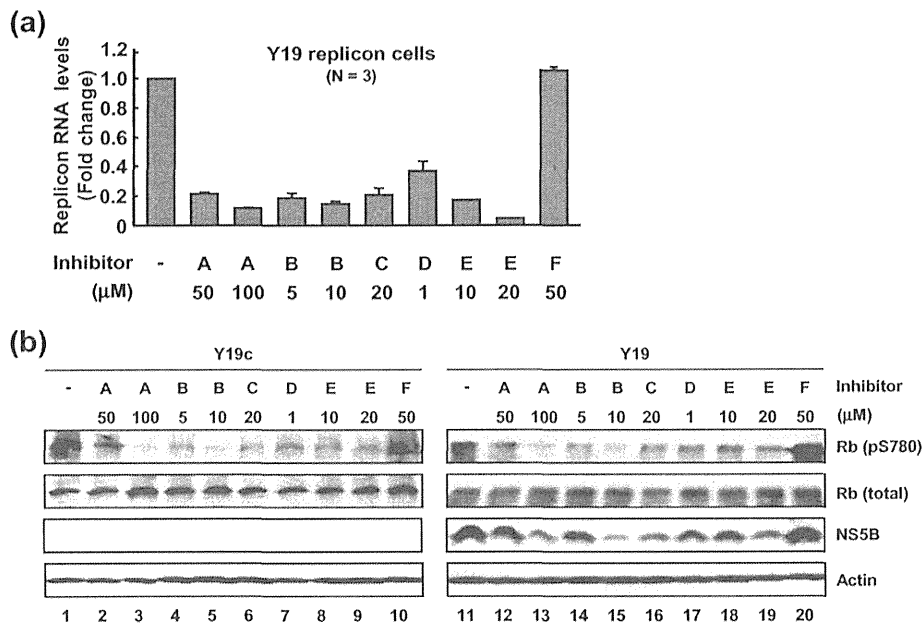1 2 3 4 5 6 7 8 9 10   11 12 13 14 15 16 17 18 19 20

Fig. 2. CDK inhibitors suppress replication of HCV genotype 2a replicon. (a) Inhibition of expression of HCV replicon RNA levels in Y19 cells. After addition of CDK inhibitor, total RNA was isolated, and HCV replicon RNA levels were quantified by real-time RT-PCR. Data represent means ± SD from three experiments. (b) Inhibition of the production of HCV protein levels in Y19 cells. After addition of CDK inhibitor, total protein was isolated and subjected to immunoblot analysis for HCV NS5B, Rb (pS780), total Rb, and actin. CDK inhibitors A–E decreased the amount of phosphorylated Rb and HCV NS5B. As expected, Y19c cells did not express HCV protein.

(a) Huh7.5.1+JFH-1 (N = 4)

HCV RNA levels (Fold change)

Inhibitor	-	A	A	B	B	C	D	E	E	F
(µM)		50	100	5	10	20	1	10	20	50

(b)

Inhibitor B
⊣
CDK4/Cyclin D
⊣
Rb
⊣
HCV

(c) HCV replicon
↓
siRNA transfection
↓ 24 hr
CDK inhibitor treatment
↓ 48hr
Assays

(d) NT siControl siRb

Rb
Actin

1 2 3

(e) HCV replication (%)
p<0.01
p<0.01

Cell viability (%)

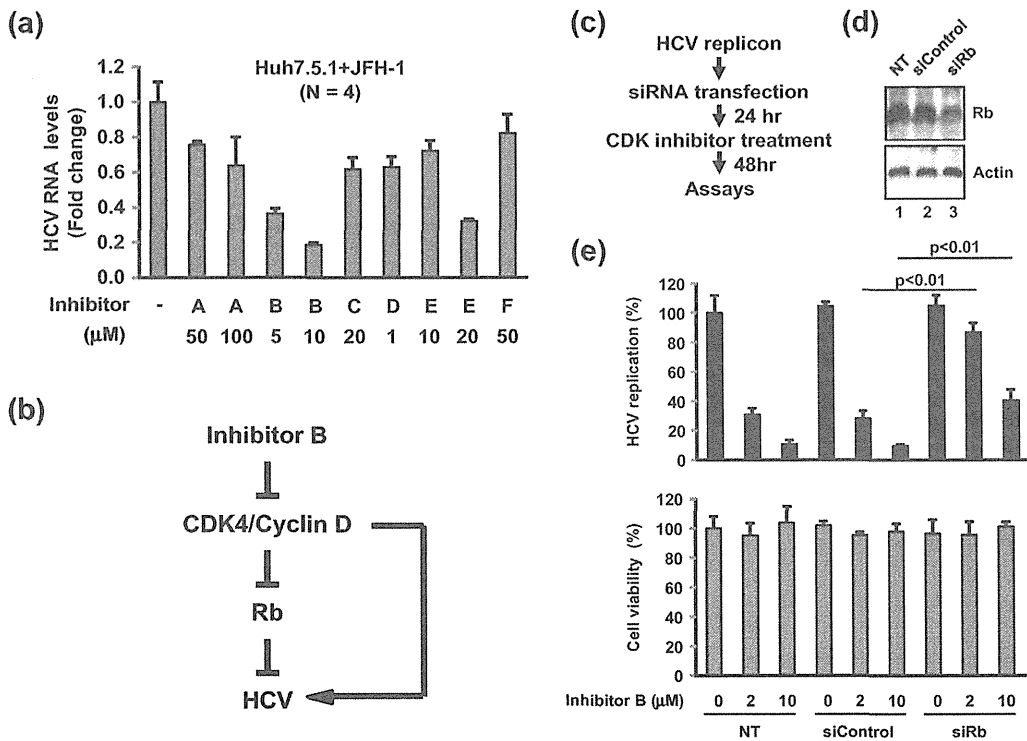| Inhibitor B (µM)	0	2	10	0	2	10	0	2	10
	NT			siControl			siRb		

Fig. 3. CDK inhibitors suppress HCV infection in cultured hepatocytes. (a) Inhibition of the expression of HCV genome RNAs in Huh7.5.1 + JFH-1 cells. After addition of CDK inhibitor, total RNA was isolated, and HCV RNA levels were quantified by real-time RT-PCR. Data represent means ± SD from three experiments. (b) Schematic of the roles of CDK inhibitor B in regulation of HCV. Under standard conditions, CDK4 phosphorylates and counteracts Rb, so permitting HCV replication; CDK4 also may play roles independently of Rb. (c) Protocol for rescue assay of CDK inhibitor treatment by Rb knockdown. (d) Immunoblot analysis of endogenous Rb. Knockdown of Rb by RNAi (40 nM) is shown. (e) Attenuation of inhibitor B-dependent suppression of HCV replication. Top panel, HCV replication; bottom panel, cell viability. Decreased HCV replication levels were partially restored by Rb knockdown. Data represent means ± SD from four independent experiments.